

December 2017

The Effects of Exhaust Vent Location on Thermal Comfort Inside the Residential Buildings Equipped With an Evaporative Cooling System

Armin Saraei

University of Nevada, Las Vegas, aminsaraei70@gmail.com

Follow this and additional works at: <https://digitalscholarship.unlv.edu/thesesdissertations>

 Part of the [Mechanical Engineering Commons](#)

Repository Citation

Saraei, Armin, "The Effects of Exhaust Vent Location on Thermal Comfort Inside the Residential Buildings Equipped With an Evaporative Cooling System" (2017). *UNLV Theses, Dissertations, Professional Papers, and Capstones*. 3167.

<https://digitalscholarship.unlv.edu/thesesdissertations/3167>

This Thesis is brought to you for free and open access by Digital Scholarship@UNLV. It has been accepted for inclusion in UNLV Theses, Dissertations, Professional Papers, and Capstones by an authorized administrator of Digital Scholarship@UNLV. For more information, please contact digitalscholarship@unlv.edu.

THE EFFECTS OF EXHAUST VENT LOCATION ON THERMAL COMFORT
INSIDE THE RESIDENTIAL BUILDINGS EQUIPPED WITH AN EVAPORATIVE
COOLING SYSTEM

By

Armin Saraei

Bachelor of Science in Mechanical Engineering
Iran University of Science & Technology
2013

A thesis submitted in partial
fulfillment of the requirement for the

Master of Science - Mechanical Engineering

Department of Mechanical Engineering
Howard R. Hughes College of Engineering
The Graduate College

University of Nevada, Las Vegas

December 2017

Copyright 2018 by Armin Saraei
All Rights Reserved



Thesis Approval

The Graduate College
The University of Nevada, Las Vegas

December 1, 2017

This thesis prepared by

Armin Saraei

entitled

The Effects of Exhaust Vent Location on Thermal Comfort inside the Residential Buildings Equipped with an Evaporative Cooling System

is approved in partial fulfillment of the requirements for the degree of

Master of Science - Mechanical Engineering
Department of Mechanical Engineering

Samir Moujaes, Ph.D.
Examination Committee Chair

Kathryn Hausbeck Korgan, Ph.D.
Graduate College Interim Dean

Brendan O'Toole, Ph.D.
Examination Committee Member

William Culbreth, Ph.D.
Examination Committee Member

Samaan Laskany, Ph.D.
Graduate College Faculty Representative

ABSTRACT

THE EFFECTS OF EXHAUST VENT LOCATION ON THERMAL COMFORT INSIDE A BUILDING EQUIPPED WITH AN EVAPORATIVE COOLING SYSTEM

By

Armin Saraei

Samir F. Moujaes, PhD., P.E., Examination Committee Chair
Professor, Department of Mechanical Engineering
University of Nevada, Las Vegas

Inlet and outlet conditions, including size and location, have significant effects on the air distribution, temperature, humidity and thermal comfort in the buildings. In the current study, various strategies are presented for exhaust air vents and the effects of inlet and outlet vent locations are evaluated on providing thermal comfort in the residential and industrial buildings. To provide thermal comfort, three key factors need to be investigated based on ASHRAE standard 55- 2013 as follows: Comfort Zone, Thermal Sensation and Draft Rate. Flow distribution is studied as well in order to investigate the strategies, which make more vorticity in the ventilated air in living spaces as a factor of increasing discomfort in the building. The case study is located in Las Vegas where the weather is hot and dry in the summer time and the relative humidity is less than 8 %. In this regard, an evaporative cooling system is considered to increase humidity in the building since not only lack of humidity cause discomfort but also has many effects on breathing and skin dryness.

A Computational Fluid Dynamic (CFD) study is developed as a numerical solution for obtaining temperature profile, relative humidity profile in different sections of the building

regarding the evaluation of Thermal comfort in most critical spaces. In this study, relative humidity definition is formulated and imported as a field function in STAR-CCM+ to track relative humidity in each points of the building. As the temperature of ventilated air increases by absorbing heat, the percentage of relative humidity will be decreased consequently inside the building. By evaluating various strategies of exhaust vents in different hours of the day, it can be concluded that the thermal comfort will be provided most appropriate if the exhaust vents in each room are on the intersection of ceiling with the middle of farthest walls from the room's entrance in a building with a single evaporative cooler.

The results presented in this study can be used in the design of air conditioning systems in residential and industrial buildings, which leads to improvement in performance of air conditioning systems without any extra expenses.

ACKNOWLEDGMENTS

This effort would have not been possible without the support of my professors at University of Nevada Las Vegas. I am especially indebted to Dr. Samir Moujaes, my advisor at University of Nevada Las Vegas and Dr. Brendan O'Toole, Chairman of the Department of Mechanical Engineering, who have been supportive of my career goals and worked actively to provide me with the protected academic time to pursue my research goals. Gratitude is extended to my thesis committee, Dr. William Culbreth and Dr. Saaman Ladkany for their tremendous supports. I am grateful to Joan Conway who helped me through the tough times. Also, I would like to thank all my friends for their supports and encouragement.

Nobody has been more important to me in the pursuit of this project than my family. I would like to thank my parents, whose love and guidance are always with me, my sister who supports and encourages me in every single moment of this journey, and my love who provides unending inspiration.

TABLE OF CONTENTS

| | |
|---|------|
| ABSTRACT..... | iii |
| ACKNOWLEDGMENTS | v |
| TABLE OF CONTENTS..... | vi |
| LIST OF TABLES..... | viii |
| LIST OF FIGURES | ix |
| CHAPTER 1: INTRODUCTION | 1 |
| 1.1. Background..... | 1 |
| 1.2. Evaporative Coolers..... | 4 |
| 1.2.1 Direct Evaporative cooler | 4 |
| 1.2.2 Indirect Evaporative Cooler | 5 |
| 1.2.3 Evaporative Cooling Calculation | 5 |
| 1.3 Thermal Comfort | 7 |
| 1.3.1 Thermal Sensation..... | 7 |
| 1.3.2 Summer and Winter Comfort Zone..... | 8 |
| 1.3.3 Draft Rate..... | 10 |
| 1.4 Objective..... | 11 |
| 1.5 Literature Review..... | 11 |
| CHAPTER 2: COMPUTATIONAL FLUID DYNAMICS (CFD) | 16 |
| 2.1 Methodology | 16 |
| 2.1.1 Software | 16 |
| 2.1.2 Governing Equations..... | 18 |
| 2.2 Characteristics of Turbulent Flow..... | 20 |
| 2.2.1 Wall Treatment | 22 |
| 2.2.2 Turbulence Modeling..... | 24 |
| 2.3 Final Remarks | 26 |
| CHAPTER 3: CFD MODEL DESCRIPTION | 27 |
| 3.1. 3D CAD Model..... | 27 |
| 3.2 Flow Field Models | 27 |
| 3.2.1. Equation of State Model | 27 |
| 3.2.2. Fluid Model..... | 28 |
| 3.3 Heat Transfer Models..... | 29 |
| 3.3.1. Solar Load Calculation Model | 29 |

| | | |
|---|---|----|
| 3.3.2. | Heat Transfer Model | 30 |
| 3.4. | Grid Generation | 30 |
| 3.4.1. | Surface Wrapper | 32 |
| 3.4.2 | Automated Mesh | 33 |
| CHAPTER 4: PROBLEM DEFINITION AND BOUNDARY CONDITIONS | | 36 |
| 4.1 | Problem Description | 36 |
| 4.2 | Surface Boundary Conditions | 40 |
| 4.2.1 | Ambient Environment Condition | 40 |
| 4.2.2 | Dimension Details | 40 |
| 4.2.3 | Materials Properties | 41 |
| 4.2.4 | Roof and Ceiling Properties | 43 |
| 4.2.5 | Inlet Condition | 43 |
| 4.2.6 | Exhaust Air Vents Condition | 46 |
| CHAPTER 5: RESULTS AND DISCUSSION | | 47 |
| 5.1 | Grid Independence Study | 47 |
| 5.2 | Wall Treatment Y+ | 49 |
| 5.3 | Residual | 51 |
| 5.4 | Validation of Results | 51 |
| 5.5 | Mass Conservation | 52 |
| 5.6 | Temperature in Different Strategies | 53 |
| 5.6.1 | Temperature Distribution | 53 |
| 5.6.2 | Temperature Profiles in Two Main Sections | 58 |
| 5.7 | Humidity Track | 61 |
| 5.8 | Thermal Comfort | 67 |
| 5.8.1 | Summer Comfort Zone Evaluation | 68 |
| 5.8.2 | Thermal Sensation | 70 |
| 5.8.3 | Draft Rate Evaluation | 72 |
| CHAPTER 6: CONCLUSION AND SUGGESTIONS | | 77 |
| 6.1 | Conclusion | 77 |
| 6.2 | Further Work | 79 |
| REFERENCES | | 81 |
| CURRICULUM VITAE | | 84 |

LIST OF TABLES

| | |
|--|----|
| Table 1. 1 Equations for Thermal Sensation Y Prediction | 7 |
| Table 1. 2. Thermal Sensation Scale..... | 8 |
| Table 2. 1. Turbulent Flow Equations Each Section of the Building..... | 21 |
| Table 2. 2. The Most Common Turbulence Models in CFD Simulation Software. | 24 |
| Table 4. 1. Building General Details..... | 41 |
| Table 4. 2. Details of the External Walls. | 42 |
| Table 4. 3. Details of the External Doors and Windows..... | 42 |
| Table 4. 4. Details of the Roof and Ceiling. | 42 |
| Table 5. 1. Mesh Properties Used for Grid Independency. | 48 |
| Table 5. 2 Mean temperature (K) - The result of the Present Work and Reference [26]..... | 52 |
| Table 5. 3 Mass Conservation of Current Study..... | 53 |
| Table 5. 4. Values of the Incident Solar Radiation on the Building. | 54 |
| Table 5. 5 Antoine Equation Constants. | 62 |
| Table 5. 6. Average Temperature and Humidity for Blocks with 2 m Height..... | 68 |
| Table 5. 7. Mean Thermal Sensation in Critical Spaces. | 70 |
| Table 5. 8. Mean Draft Rate in Critical Spaces..... | 72 |

LIST OF FIGURES

| | |
|---|----|
| Figure 1. 1 The Schematic Picture of Direct Evaporative Cooler [4]..... | 5 |
| Figure 1. 2 Cooling Processes Representation in Psychrometric Chart..... | 6 |
| Figure 1. 3 ASHRAE Summer and Winter Comfort Zones [1]..... | 9 |
| Figure 1. 4 Thermal Comfort Adaptive Model [10]. | 12 |
| Figure 1. 5 Skin Temperature Distribution Over Human Body [11]. | 12 |
| Figure 2. 1 Wall Treatment..... | 24 |
| Figure 3. 1 Schematic Representation of Radiation [8]..... | 29 |
| Figure 3. 2 Schematic Representation of Environment Model [8] | 30 |
| Figure 3. 3 Different Types of Mesher in STAR-CCM+..... | 31 |
| Figure 3. 4 Capturing the Indoor Air Using Surface Wrapper..... | 32 |
| Figure 3. 5 The Effects of Using Surface Remesher..... | 33 |
| Figure 3. 6 Volume Mesh with 5 Prism Layers | 35 |
| Figure 4. 1 Flow Geometry and Solution Field (Perspective View)..... | 36 |
| Figure 4. 2 Flow Geometry and Solution Field Parallel Views:..... | 37 |
| Figure 4. 3 Flow Geometry and Solution Field (Inside View) | 38 |
| Figure 4. 4 Strategies of Exhaust Vent Locations..... | 39 |
| Figure 4. 5 Floor Plan (inch)..... | 41 |
| Figure 5. 1. Evaluation of Grid Independency In Terms of Temperature and Velocity. | 47 |
| Figure 5. 2. Temperature Independency. | 48 |
| Figure 5. 3. Velocity Independency. | 49 |
| Figure 5. 4. Wall Treatment (Y+). | 50 |
| Figure 5. 5. Wall Y+ Distribution (1,106,431 cells). | 50 |
| Figure 5. 6. Residual Monitor of the Current Study | 51 |

| | |
|--|----|
| Figure 5. 7. Strategy A: Temperature Distribution in..... | 54 |
| Figure 5. 8. Strategy B: Temperature Distribution. | 55 |
| Figure 5. 9. Strategy C: Temperature Distribution. | 56 |
| Figure 5. 10. Strategy D: Temperature Distribution. | 57 |
| Figure 5. 11. Study Sections Through the Building for Temperature Profile Evaluation..... | 58 |
| Figure 5. 12. Temperature Profiles of Various Strategies at Section 1..... | 59 |
| Figure 5. 13. Temperature Profiles of Various Strategies at Section 2..... | 60 |
| Figure 5. 14. Relative Humidity Tracking in the Entire of the House for Various Strategies. | 63 |
| Figure 5. 15. Relative Humidity Profiles of Various Strategies at Section 1..... | 64 |
| Figure 5. 16. Relative Humidity Profiles of Various Strategies at Section 2..... | 65 |
| Figure 5. 17. Critical Spaces for Thermal Comfort Evaluation. | 67 |
| Figure 5. 18. ASHRAE Summer Comfort Zones for Bedroom 1..... | 69 |
| Figure 5. 19. ASHRAE Summer Comfort Zones for Bedroom 2..... | 69 |
| Figure 5. 20. ASHRAE Summer Comfort Zones for Bedroom 3..... | 70 |
| Figure 5. 21. Thermal Sensation In the 4 Strategies. | 71 |
| Figure 5. 22. Draft Rate in the Various Strategies. | 73 |
| Figure 5. 23. Velocity Vector in Bedroom 1 (Top View)..... | 74 |
| Figure 5. 24. Velocity Vector in Bedroom 2 (Top View)..... | 75 |
| Figure 5. 25. Velocity Vector in Bedroom 3(Top View)..... | 76 |

CHAPTER 1

INTRODUCTION

1.1. Background

After the Industrial revolution, the invention of systems related to heating, ventilation, and air conditioning (HVAC) has begun all over the world. The relation between heating, ventilation and air conditioning caused efforts to provide thermal comfort in buildings, the acceptable indoor air quality and logical maintenance expenses. These systems worked based on the concept of reduction of air infiltration and maintaining the pressure in different sections of buildings. The collection and distribution of ventilated air in the space has been recognized as a definition under the title of “Air distribution”. The global investments in this industry are based on making job opportunities for maintenance, design, and manufacturing; sales markets; education; and research.

Ventilation and air conditioning is a process regarding controlling temperature and humidity, eliminating unpleasant smells, dust and bacteria by injecting fresh air and making air flow into the building. Air conditioning systems are used to eliminate extra heat from the spaces and this is the most basic responsibility of an air conditioner. However, in hot and dry climate, the typical air conditioning systems cannot provide appropriate ventilated air for the building. Due to lack of humidity in these climates, it is necessary to provide humidified ventilated air to maintain comfortable situation for residents since the lack of humidity in the air causes some problems such as skin and hair dryness, respiratory illness, etc. Although some efforts have been made to increase the humidity of air in vapor-compression cycle air conditioners, one of the most

common ways is the using of evaporative cooling systems. Evaporative coolers work based on the exchange of sensible heat for latent heat and cool down the air by the evaporation of water.

In another side, providing comfort for residents of buildings is one of the most important necessities since people spend more than 90 % of their lives inside buildings. In this regard, the ASHRAE Standard 55 [1] introduces the factors, which most affect the thermal comfort. Based on this standard, thermal comfort is influenced by below factors:

1. Temperature

One of the parameters, which play a key role in thermal comfort is the temperature range inside the building. The temperature could range from 19 to 28°C (67-82°F). A more specific range can be determined from ASHRAE standard 55, notes that the temperature range depends on relative humidity, season, clothing worn, activity levels, etc. [1].

2. Humidity

Low level of relative humidity (Below 25%) is a reason to provide discomfort in buildings. It causes skin drying, irritation and increases electricity, which causes discomfort. On the other hand, a high level of humidity increases the chance of emerging molds and fungi. In this regard, the relative humidity should be kept lower than 65% to reduce the likelihood of conditions that can lead to microbial growth [2].

3. Air Movement

Air movement is one of the other important factors in thermal comfort, which is typically defined as the rate of air movement. According to ASHRAE standard 55, the rate of air movement is equal to the average speed of the air, which the human body is exposed based on the location of the building and time and it should be less than 1.2m/s.

4. Activity

Since people may have different activities in each section of the building, the condition for providing thermal comfort in each space is disparate based on its usage. ASHRAE standard 55 provides a table of metabolic rate for a variety activities and declares how much heat will be produced by the human body based on the kind of activity.

5. Clothing

Clothing is a thermal insulation and therefore the clothes worn by a resident impacts thermal comfort since it affects the heat loss and thermal balance in the building.

It is necessary to have information about velocity, pressure, turbulence intensity, temperature and relative humidity in each section of the building to be able to provide thermal comfort in all sections. Although experimental experiences allow us to get very useful results to use as a basis for designing, we need some other tools to be able to find air movement model, velocity and temperature profile in each section of the building, which is not possible to get experimentally.

In this project, a 3-D computational fluid dynamic (CFD) model has been used to simulate the distribution of ventilated air in a building and effects of the exhaust vents locations on providing thermal comfort in each section. By using CFD simulation, not only can we get temperature profile in each section of the building, but we will be able to track relative humidity in each point needed to be considered, air velocity, turbulence effects in the flow pattern and monitor pressure to make sure that the thermal comfort has been dominated in each section of the building.

1.2 Evaporative Coolers

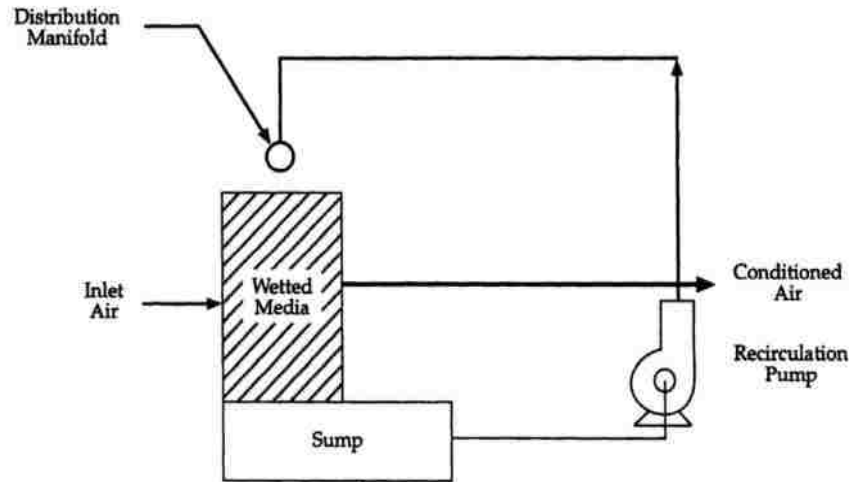
Nowadays, one of the biggest concerns is decreasing energy consumption in the buildings, and we face new challenges to develop innovative efficient machines to decrease the environmental impacts of air conditioning systems.

It has been estimated that around 20% of energy consumption has been dedicated to heating and cooling systems of residential and industrial buildings. Most of recent HVAC systems work based on the vapor-compression refrigeration cycle, which use Chlorofluorocarbons (CFCs) and Hydro chlorofluorocarbons (HCFCs) as the refrigerants. Using these kinds of systems highly increase the energy consumption of nonrenewable energies. As an alternative trustful system considered for decreasing the above-mentioned impacts is using an evaporative cooling system to address the necessity of heating and cooling of buildings [3].

Evaporative air-conditioning (EAC) relies on water as a coolant rather than on chemical refrigerant, which has important environmental and economic benefits. EAC can provide perfect cooling and ventilation under the right condition, which minimizes energy consumption and humidifies the air which is necessary especially in hot and dry climate.

1.2.1 Direct Evaporative cooler

Direct EAC is the most common and traditional form of air conditioning, which typically uses a fan to move outside hot air into a porous wetting medium. Heat will be absorbed by the water since it will be evaporated from the porous medium and the air temperature will drop as it leaves the EAC. One of the most important concerns in EAC is the use of water. There are variant needs of water based on the size of the cooler from a few liters per day up to a hundred liters or more.



1.2.2 Indirect Evaporative Cooler

The indirect evaporative cooler is a method, which cools down air more than direct evaporative ones. These effects can be accomplished by adding an additional step into the cooling process. In other words, the inlet air is cooled first in an air-to-air heat exchanger, which is called indirect since it doesn't add moisture to the supply air. Instead, only one side of the heat exchanger is in contact with evaporating water as the supply air passes through the other side, which causes the temperature drops and then, as it goes through the direct EAC stage, it will be moisturized. Usually, the final air temperature at the outlet of an indirect cooler is 3.5 °C (6.3°F) cooler than what is achievable from direct evaporative coolers [4].

1.2.3 Evaporative Cooling Calculation

Generally, the cooling processes are represented in the psychrometric chart. Psychrometric chart is a graphical representation of the physical properties of air such as dry and wet bulb air temperature, relative humidity and humidity ratio (Specific Humidity), enthalpy,

density, etc. Typically, the cooling process is classified into two groups: 1. Sensible Cooling and 2. Evaporative Cooling as it is represented in Figure 1.2.

In the sensible cooling process, the temperature of air changes (as shown in Fig 1.2) while the humidity ratio is maintained. In this process, when the dry bulb temperature is reduced, the wet bulb temperature is also reduced; however, the humidity ratio is constant since there is no addition or loss of moisture.

On the other hand, in evaporating cooling process, both dry bulb temperature and the humidity ratio of air changes along the lines of constant enthalpy and wet bulb temperature. There is no change in heat content in air and the energy is converted from sensible to latent form.

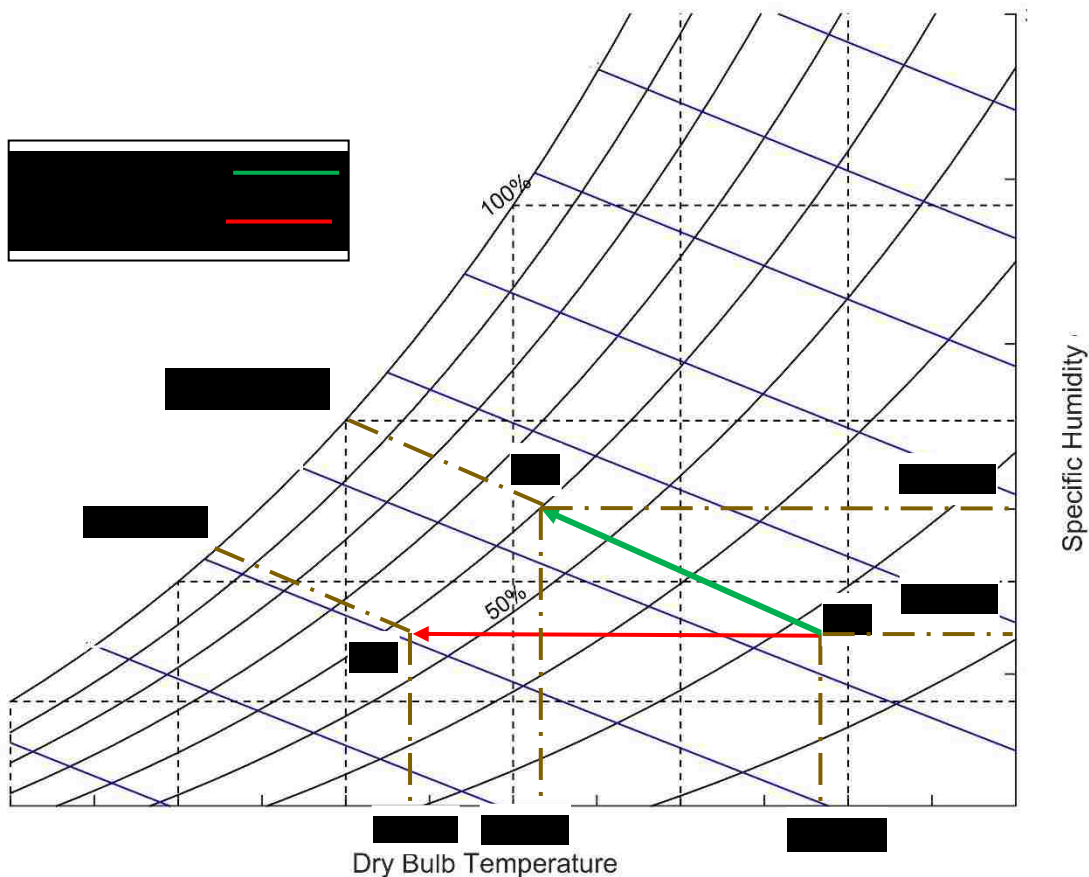


Figure 1. 2 Cooling Processes Representation in Psychrometric Chart.

As it is shown in Figure 1.2, in the evaporative cooling process, changes occur in dry bulb temperature, density, humidity ratio, relative humidity and the vapor pressure of the moist air; however, there is no change in **Enthalpy** and **Wet bulb temperature**.

1.3 Thermal Comfort

As it has been discussed in section 1.1, Thermal comfort is the condition when thermal satisfaction is dominant in the environment. Besides environmental and personal factors mentioned in section 1.1, other factors are also considered to provide comfort, which includes nonuniformity of the environment, visual stimuli, age and outdoor climate [1]. However, there are three main factors, which are more important and needed to be considered to verify thermal comfort in the building as follows:

1.3.1 Thermal Sensation

Thermal sensation is calculated by correlations between comfort level, temperature, humidity, gender, and length of exposure as shown in Figure 1.3.

Table 1. 1 Equations for Thermal Sensation Y Prediction

| Exposure Period, h | Subjects | Regression Equations |
|--------------------|----------|--|
| | | t= dry- bulb temperature, °C p= vapor pressure, kPA |
| 1.0 | Men | $Y=0.220 t+0.233 p-5.673$ |
| | Women | $Y=0.272 t+0.248 p-7.245$ |
| | Both | $Y=0.245 t+0.248 p-6.475$ |
| 2.0 | Men | $Y=0.221 t+0.270 p-6.024$ |
| | Women | $Y=0.283 t+0.210 p-7.694$ |
| | Both | $Y=0.252 t+0.240 p-6.859$ |
| 3.0 | Men | $Y=0.212 t+0.293 p-5.949$ |
| | Women | $Y=0.275 t+0.255 p-8.622$ |
| | Both | $Y=0.243 t+0.278 p-6.802$ |

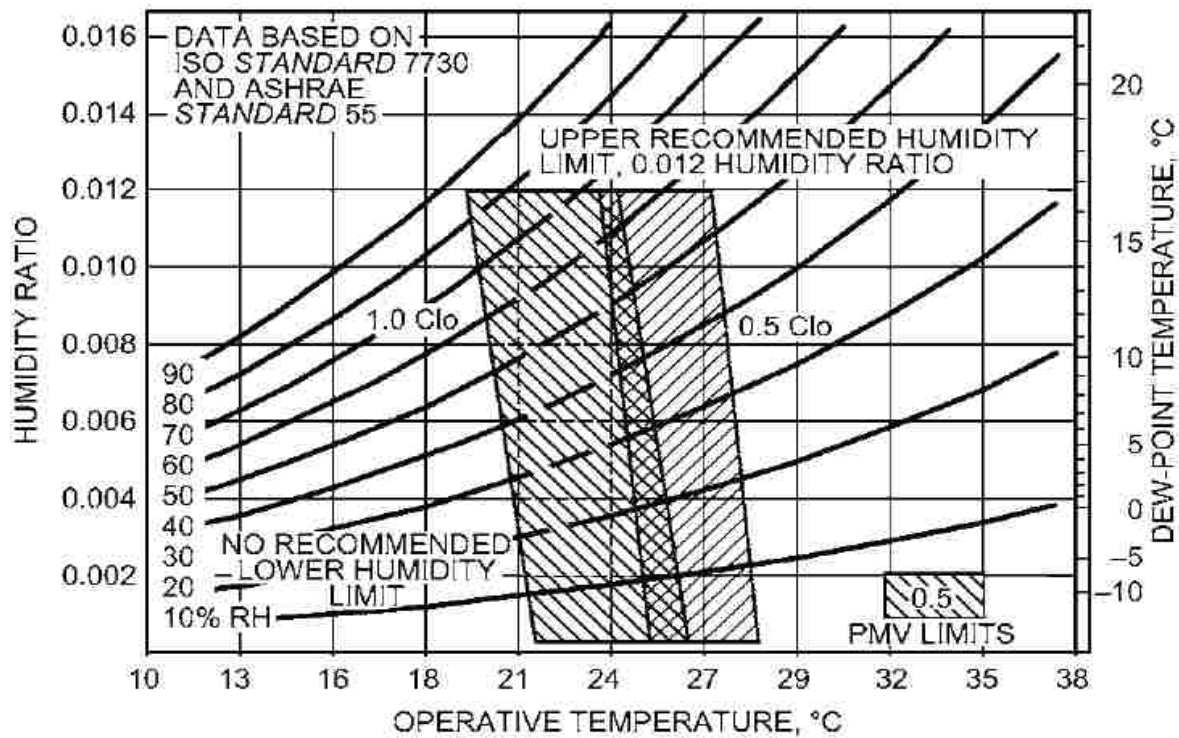
A thermal sensation scale is developed in which neutral mode would be the ideal condition for providing thermal comfort in the environment. In the current study, the exposure period is assumed to be 1 hour for **both men and women**. The ASHRAE standard 55 has a scale for thermal sensation, which is represented in Table 1.1.

Table 1. 2. Thermal Sensation Scale.

| | |
|----|---------------|
| +3 | Hot |
| +2 | Warm |
| +1 | Slightly warm |
| 0 | Neutral |
| -1 | Slightly cool |
| -2 | Cool |
| -3 | Cold |

1.3.2 Summer and Winter Comfort Zone

Since people wear different levels of clothing based on the situation and weather, ASHRAE 55 [1] has defined thermal comfort zone for 0.5 and 1 clo[0.078 and 0.155 m². K/W] (0.44 and 0.88ft²h. °F/Btu) as shown in Figure 1.4. For instance, a suit has about 1 clo and a short-sleeved shirt and trouser have about 0.5 clo [1]. Therefore, the comfort zone with 0.5 clo is used for summer design. As much as the condition of the indoor air is closer to the shared part between two zones, the thermal sensation is closer to the neutral mode, which is the ideal situation as it has been represented in section 1.3.1.



ASHRAE recommends that the dew point temperature of occupied space should not be less than 36°F (2.2°C) since it causes eye discomfort. In addition, ASHRAE 55 recommends that the relative humidity should not exceed 60 % to maintain the internal air condition in the comfort zone.

To use Figure 1.4, it is necessary to obtain the Operative Temperature of the space. However, the average temperature is permitted to be used instead of operative temperature when there is no radiant panel cooling system. Since in the current study the only system considered is an Evaporative Cooler, the operative temperature is assumed to be equal to internal average air temperature.

1.3.3 Draft Rate

Draft is an undesired cooling of the human body caused by air movement. This is a serious problem in ventilated buildings, automobiles and aircrafts. When residents feel the draft, they desire higher air temperature in the space. This dissatisfaction is caused by the air velocity dominated in the space and in this regard, the mean velocity in the space is one of the important aspects needed to be considered in thermal comfort analysis of a ventilated space. The acceptable higher limit for DR should be less than 15% [1]. The Draft Rate is given by:

$$DR = (34 - t_a)(V - 0.05)^{0.62}(0.37VTu + 3.14) \quad (1.1)$$

Where,

t_a : Indoor ventilated air temperature, °C

V: Local mean air velocity, m/s

Tu: Turbulence Intensity, %

The turbulence intensity is defined as:

$$Tu = \frac{u'}{V} \quad (1.2)$$

Where,

u' : Root-mean-square of the turbulent velocity fluctuations, m/s and is calculated as follows:

$$u' = \sqrt{\frac{1}{3}(u'_x{}^2 + u'_y{}^2 + u'_z{}^2)} = \sqrt{\frac{2}{3}K} \quad \text{Where K is Turbulent Kinetic Energy}$$

V: Local mean air velocity, m/s

1.4 Objective

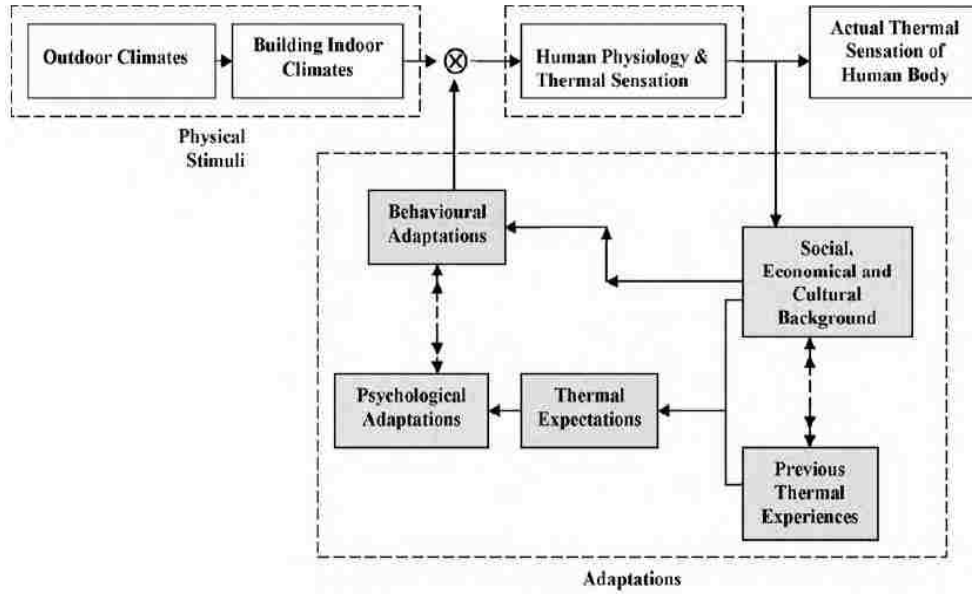
The objectives of this project are:

1. To predict the best strategy for the location of ceiling exhaust vents in the building and evaluate thermal comfort in different sections of the building.
2. To provide detailed information regarding temperature profile, humidity, velocity and the pressure in each section of the building.

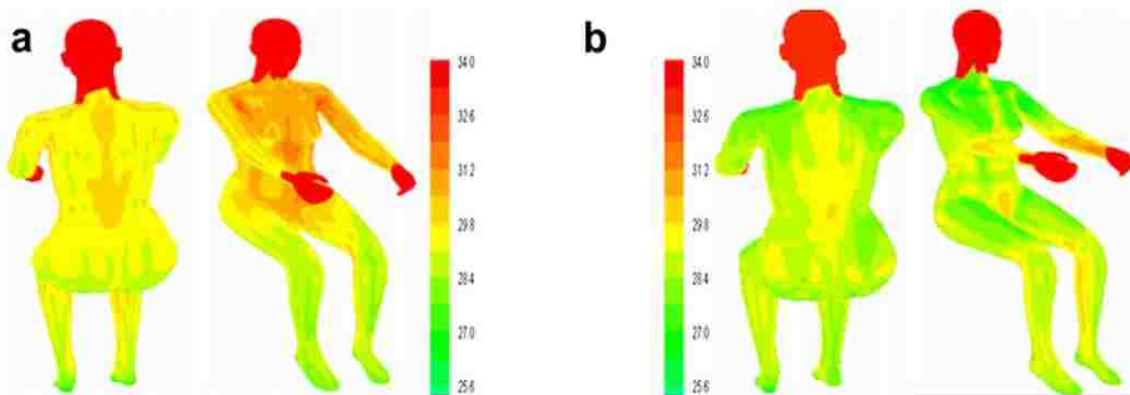
1.5 Literature Review

The energy consumption of residential buildings for ventilation and air conditioning purposes in developed countries is around 30 % of total energy consumed. A considerable amount of energy is consumed regarding **thermal comfort**, meanwhile we are facing the energy crisis all over the world. The worldwide attitude is minimizing energy consumption for thermal comfort and it causes one of the most critical concerns, which have led to abundant research in this regard.

Djongyang et al. have presented a review regarding the physiological basis of comfort by considering human body as a thermoregulatory system. The formulation of mathematical modeling of heat transfer has been recalled between the environment and the human body, considering main effects such as conduction, convection, radiation, humidity, and clothing. In addition, a theoretical model of thermal comfort has been represented, which different factors such as culture, climate, social, psychological and behavioral adaptation has been considered as parameters, which have impacts on thermal comfort [10].



Moreover, Cheng et al. [11] has considered physiological responses of the human body in his research and evaluated the thermal comfort for an indoor application using CFD simulation, and represented results including patterns of airflow and air temperature profile. In addition, skin temperature distribution has been represented and it has been concluded that the temperature will be decreased as an air supplier will be added to the model, which provides a sense of comfort in residents.



Fue et al. have represented different human thermo-regulation models regarding interacting two active (the human body) and passive systems (heat transportation between the human body and the environment). A CFD simulation has been represented to evaluate human body situation in different applications, such as thermal comfort for energy conservation purposes [12]. In addition, a number of studies are involved in how the position of air conditioning systems can help to maintain thermal comfort more appropriate in buildings, cars, aircrafts, etc. In order to deplete energy consumption, the location of inlets, exhaust air vents, air velocity at the inlet, inlet air temperature and humidity, the pressure difference between inlet and exhaust vent etc, should be considered. The strategy used in installing air conditioning systems can help to decrease desired cooling thermal load for providing thermal comfort in buildings and consequently smaller and more efficient systems will be required and lead us to eliminate unnecessary energy consumption.

Zhang et al. [13] evaluated air flow field, temperature profile and uniformity inside a passenger compartment for providing thermal comfort. Fredriksson et al. [14] performed an experimental study on a mock office, evaluated air flow and temperature and concluded that the air flow from the chilled beam is similar to a plume; however, there is strong oscillation along the chilled beam and in the sideways. Ding et al. [15] presented a computational fluid dynamic (CFD) simulation for two kinds of refrigerators to study flow fields and temperature distribution, and evaluated the results experimentally. Zingano [16] studied several experimental models to discuss the importance of humidity in providing thermal comfort. To determine the thermal comfort temperature, an indirect method is represented. Li et al. [17] have conducted an experimental study to investigate contaminant distribution in an aircraft cabin.

Another important aspect in thermal comfort is the percentage of humidity and humidity distribution in the ventilated space. Manzan and Saro [18] have evaluated temperature distribution, flow field and water vapor distribution within a duct by the numerical simulation method. Khan et al. [19] investigated the ventilation of a simple model for several different inlets and exhaust outlets location. They concluded that the exhaust outlets near the ceiling are better than exhaust outlets near the floor regarding the steady-state distribution of contaminant concentrations. Zitek et al. [20] carried out research on the thermal comfort in an aircraft. They presented a novel design to supply fresh air with a suitable range of relative humidity for each passenger individually, and each seat in the cabin had a separate inlet and exhaust system. Yang et al. [21] proposed a mathematical model of a natural draft wet cooling tower to optimize its design and its operational efficiency. Bojic et al. [22] performed a CFD simulation to predict temperature and flow distribution inside recessed spaces in which differs in heights and condenser-unit locations. Liang Pu et al. [23] also elaborated the effects of different inlet vent positions on the humidity distribution inside a room, concluding that the non-uniformity of relative humidity decreases with increasing of RH at the inlet.

Some researchers have investigated the heat and moisture transfer from/to water and air, which is the basis of creating an evaporative cooler as an environmentally-friendly tool to decrease air temperature in buildings [24]. Moreover, Sureshkumar et al. [25] worked on heat and mass transfer between a water spray and ambient air under different conditions both experimentally and numerically. However, there are few studies focusing on the effects of inlet and exhaust vent locations on the humidity distribution inside a building.

In the current study, various strategies are investigated for exhaust air vents located in the ceiling for a house with many different sections making the CFD modeling complicated. A

single direct evaporative cooler is responsible to ventilate, decrease the temperature and humidify the internal air. The evaporative cooler has only one inlet into the building, which is connected from a wall connected to the unventilated garage. The various strategies are evaluated for different hours on a summer day in hot and humid weather, and the results from the various strategies have been compared to find the most appropriate one.

CHAPTER 2

COMPUTATIONAL FLUID DYNAMICS (CFD)

2.1 Methodology

2.1.1 Software

Computational Fluid Dynamics or CFD is the analysis of systems regarding fluid flow behavior, heat transfer and specific phenomena, such as chemical reacting by taking advantages of computer-based simulation. This technique is very strong and can be expanded in the different fields such as industrial, residential or commercial applications. CFD simulation is widely used in different areas such as aerodynamic, turbomachinery, power plant, chemical process engineering, external and internal environment of buildings, etc.

Moreover, recent methods are used for designing combustion chambers and combustion engine and even vehicle manufacturer are using CFD simulation to predict drag force and air movement model around and inside the cars. To summarize, CFD is becoming one of the most important analyses needed to design components in different environments, which are dealing with different fluid flows. One of the most important reasons, which persuade us to do CFD analysis is the huge expenses of running experiments for validating the criteria of designs. CFD can produce different kinds of results based on needs with no added expenses. CFD codes basically consist of the numerical algorithms, which can deal with the fluid flow problem. In all kind of these codes, three main elements are included: 1. a pre-processor, 2. a solver and 3. a post- processor.

1. **Pre-Processor:** is consisting of the inputs used for a CFD problem and the transformation of them into a form suitable to be used with the solver.
2. **Solver:** Different numerical solution methods are available such as Finite Difference, Finite Element, Spectral methods and Finite Volume method.
3. **Post- Processing:** After getting the results, different methods are needed to analyze the results such as contour plots, vector plots, streamlines, etc.

The differences between the above-mentioned solvers are mainly associated with the way, which flow variables have been approximated and with the discretization processes.

Finite differences method: FDM is a numerical method, which solves differential equations by approximating them with differences equations. In other words, this method represents the unknown ϕ of the CFD problem by means of point samples at the node points of a grid of coordinate lines.

Finite element method: FEM uses smooth, piecewise continuous functions (linear or quadratic) to describe the local variation of unknown flow variables ϕ . For solving a problem using this method, the problem will be subdivided into smaller parts, which are called finite elements. Therefore, simpler equations, which have been used to solve finite elements, will be assembled into the larger equations that model the entire problem.

Spectral methods: In this method unlike, FDM and FEM methods, the approximation of unknowns are not local but are valid for the entire domain. In this method, the approximation of unknowns is done by using Fourier and Chebyshev polynomial series.

Finite volume method: Similar to FDE and FEM methods, the problem will be solved for small and simpler parts, which are called finite volume to have simpler equations and then it will

be assembled into larger equations to solve the entirety of the domain. Many of CFD software codes are working based on FVM method including PHENICS, FLUENT, FLOW3D, STAR-CD and Star- CCM+ [8].

STAR- CCM+ is a CFD simulation software for solving multidisciplinary problems in both fluid and solid continuum mechanics, within a single integrated user interface. Almost all of the industries involved in computational engineering solutions and CFD simulation use STAR-CCM+. The STAR-CCM+ software provides all stages needed for CFD analysis in every industry including aerospace, building energy analysis, rotational and centrifugal devices, heat exchangers, computer parts heat analysis, etc. These features are including [9]:

- Import and creation of geometries
- Mesh generation
- Solution of governing equations
- Automation of the simulation workflows for design exploration studies
- Connection to other Computational Aided Engineering (CAE) software for co-simulation analysis

2.1.2 Governing Equations

To solve a problem related to heat transfer and fluid flow, it is necessary to solve governing equations of fluid flow, which represents mathematical statements of the conservation laws of physics. In this project, we need to evaluate thermal comfort inside the building while the turbulence and buoyancy effects should be considered. Generally, the indoor air has been assumed to be an ideal multi-components and turbulent. The governing equations of this kind of

flow depend on mass conservation, momentum, and energy conservation equations. The conservation equations are used to model the behavior of fluid film.

Conservation of Mass Equation (Continuity):

The rate of increase of mass in fluid element should be equal to the net rate of flow of mass into the fluid element [8].

$$\frac{\partial(\rho)}{\partial t} + \frac{\partial(\rho u)}{\partial x} + \frac{\partial(\rho v)}{\partial y} + \frac{\partial(\rho w)}{\partial z} = 0 \quad (2.1)$$

Conservation of Momentum Equations:

Conservation of momentum equations are based on Newton's second law, which states that the rate of increase in momentum of the fluid particle in each direction should be equal to the sum of forces on the fluid particle in the same direction [8]. Two types of forces are considered on fluid particles:

1. **Surface forces:** which includes pressure and viscous forces.
2. **Body forces:** which includes gravity, centrifugal, Coriolis and electromagnetic forces.

The three equations for Newtonian fluid in Cartesian coordinates are represented as follows:

$$\rho\left(\frac{\partial u}{\partial t} + u\frac{\partial u}{\partial x} + v\frac{\partial u}{\partial y} + w\frac{\partial u}{\partial z}\right) = \rho g_x - \frac{\partial p}{\partial x} + \mu\left(\frac{\partial^2 u}{\partial x^2} + \frac{\partial^2 u}{\partial y^2} + \frac{\partial^2 u}{\partial z^2}\right) \quad \text{X-Direction (2.2)}$$

$$\rho\left(\frac{\partial v}{\partial t} + u\frac{\partial v}{\partial x} + v\frac{\partial v}{\partial y} + w\frac{\partial v}{\partial z}\right) = \rho g_y - \frac{\partial p}{\partial y} + \mu\left(\frac{\partial^2 v}{\partial x^2} + \frac{\partial^2 v}{\partial y^2} + \frac{\partial^2 v}{\partial z^2}\right) \quad \text{Y-Direction (2.3)}$$

$$\rho\left(\frac{\partial w}{\partial t} + u\frac{\partial w}{\partial x} + v\frac{\partial w}{\partial y} + w\frac{\partial w}{\partial z}\right) = \rho g_z - \frac{\partial p}{\partial z} + \mu\left(\frac{\partial^2 w}{\partial x^2} + \frac{\partial^2 w}{\partial y^2} + \frac{\partial^2 w}{\partial z^2}\right) \quad \text{Z- Direction (2.4)}$$

Where

ρ =density

g_x, g_y, g_z =body forces

μ =viscosity

p =hydrostatic pressure

t =time

Conservation of Energy Equation:

The energy equation is based on the first law of thermodynamics, which states that the rate of increase of energy in the fluid particle should be equal to the net rate of heat added to the fluid particle plus the net rate of work done on the particle [8].

$$\rho c_p \left(\frac{\partial T}{\partial t} + u \frac{\partial T}{\partial x} + v \frac{\partial T}{\partial y} + w \frac{\partial T}{\partial z} \right) = k \left(\frac{\partial^2 T}{\partial x^2} + \frac{\partial^2 T}{\partial y^2} + \frac{\partial^2 T}{\partial z^2} \right) + \mu \varphi \quad (2.5)$$

$$\varphi = 2 \left[\left(\frac{\partial u}{\partial x} \right)^2 + \left(\frac{\partial v}{\partial y} \right)^2 + \left(\frac{\partial w}{\partial z} \right)^2 \right] + \left(\frac{\partial u}{\partial x} + \frac{\partial v}{\partial y} \right)^2 + \left(\frac{\partial v}{\partial z} + \frac{\partial w}{\partial y} \right)^2 + \left(\frac{\partial w}{\partial x} + \frac{\partial u}{\partial z} \right)^2 - \frac{2}{3} \left(\frac{\partial u}{\partial x} + \frac{\partial v}{\partial y} + \frac{\partial w}{\partial z} \right)^2 \quad (2.6)$$

Where

c_p =specific heat at constant pressure

k =thermal conductivity

φ =dissipation function

2.2 Characteristics of Turbulent Flow

The crucial difference between laminar and turbulent flow is emerging eddy motion and dissipation in the turbulent fluid flow. When the value of Reynolds number is above Re_{cr} , a different kind of event will take place, which leads to a radical change of the flow character and the flow behavior becomes chaotic. This regime, which is called turbulence, is one of the most

important aspects of the fluid mechanics since in reality we are dealing with turbulence flow in different environments. Because of buoyancy effects in boundary conditions and diffusion near the walls, we need to use the turbulent model to solve the flow behavior near the walls, which completely affects the heat transfer, velocity, and pressure in different parts of the building.

Since the relative humidity of the inlet air will decrease as it heats up when it goes through the different sections of the building, the density of air is different in each part of the building. Therefore, the mean density may vary and always exhibit turbulent fluctuation. The behavior of flow is close to the definition of ideal gases. Therefore, the air will be assumed to be an ideal gas. As it is represented in Table 2.1, the density-weighted averaged form of the mean flow equations for turbulent flow with variable density (which has been used in CFD simulation software) is as follows:

Table 2. 1. Turbulent Flow Equations For A Flow With Variable Density In Each Section Of The Building.

| | | |
|---------------------------|--|--------|
| Continuity | $\frac{\partial \rho}{\partial t} + \text{div}(\rho U) = 0$ | (2.6) |
| Reynolds equations | $\frac{\partial(\rho U)}{\partial t} + \text{div}(\rho U U) = -\frac{\partial P}{\partial x} + \text{div}(\mu \text{grad} U) + \left[-\frac{\partial(\overline{\rho u'^2})}{\partial x} - \frac{\partial(\overline{\rho u'v'})}{\partial y} - \frac{\partial(\overline{\rho u'w'})}{\partial z} \right] + S_{Mx}$ | (2.7) |
| | $\frac{\partial(\rho V)}{\partial t} + \text{div}(\rho V U) = -\frac{\partial P}{\partial y} + \text{div}(\mu \text{grad} V) + \left[-\frac{\partial(\overline{\rho u'v'})}{\partial x} - \frac{\partial(\overline{\rho v'^2})}{\partial y} - \frac{\partial(\overline{\rho u'w'})}{\partial z} \right] + S_{My}$ | (2.8) |
| | $\frac{\partial(\rho W)}{\partial t} + \text{div}(\rho W U) = -\frac{\partial P}{\partial z} + \text{div}(\mu \text{grad} W) + \left[-\frac{\partial(\overline{\rho u'w'})}{\partial x} - \frac{\partial(\overline{\rho v'w'})}{\partial y} - \frac{\partial(\overline{\rho w'^2})}{\partial z} \right] + S_{Mz}$ | (2.9) |
| Scalar transport equation | $\frac{\partial(\rho \phi)}{\partial t} + \text{div}(\rho \phi U) = -\frac{\partial P}{\partial x} + \text{div}(\mu \text{grad} \phi) + \left[-\frac{\partial(\overline{\rho u'\phi'})}{\partial x} - \frac{\partial(\overline{\rho v'\phi'})}{\partial y} - \frac{\partial(\overline{\rho w'\phi'})}{\partial z} \right] + S_{\phi}$ | (2.10) |

2.2.1 Wall Treatment

Typically, walls are one of the important sources in producing vorticity in most of the flow problems. Therefore, a good prediction of the flow behavior and turbulent parameters across the wall boundary layer is an essential concern.

The boundary layer will be divided into three sublayers. The flow has different characteristics in each layer as follows:

1. Viscous sublayer

The flow when it is in contact with the wall is almost laminar because the viscous effects are dominant. The mean flow velocity completely depends on the distance from the wall, shear stress, viscosity and the fluid density. The fluid should be stationary at the wall surface. Therefore, turbulence must stop very close to the walls, and the shear stress is dominated by viscous shear.

The thickness of this layer is extremely thin ($y^+ < 5$), and it can be assumed that the shear stress is constant and equal to wall shear stress throughout the layer. Therefore:

$$u^+ = y^+ \quad (2.11)$$

Note that:

$$y^+ = \frac{yu_\tau}{\nu} \quad (2.12)$$

And

$$u^+ = \frac{u}{u_\tau} \quad (2.13), \quad u_\tau = \sqrt{\frac{\tau_w}{\rho}} \quad (2.14)$$

Where:

y : Normal distance from the wall to the wall-cell centroid

u : Velocity parallel to the wall

ν : Kinematic viscosity

u_τ : Friction Velocity

τ_w : Wall Shear Stress

ρ : Fluid Density

2. Log-Law layer

This layer is dominated by both viscous and turbulent effects. In this layer, which is out of viscous sublayer ($30 < y^+ < 500$), the shear stress varies with the distance from the wall, and it is assumed to be constant and equal to the wall shear stress.

$$u^+ = \frac{1}{k} \ln y^+ + B = \frac{1}{k} \ln(Ey^+) \quad (2.14)$$

Where the numerical values for the constants are:

$K=0.4$

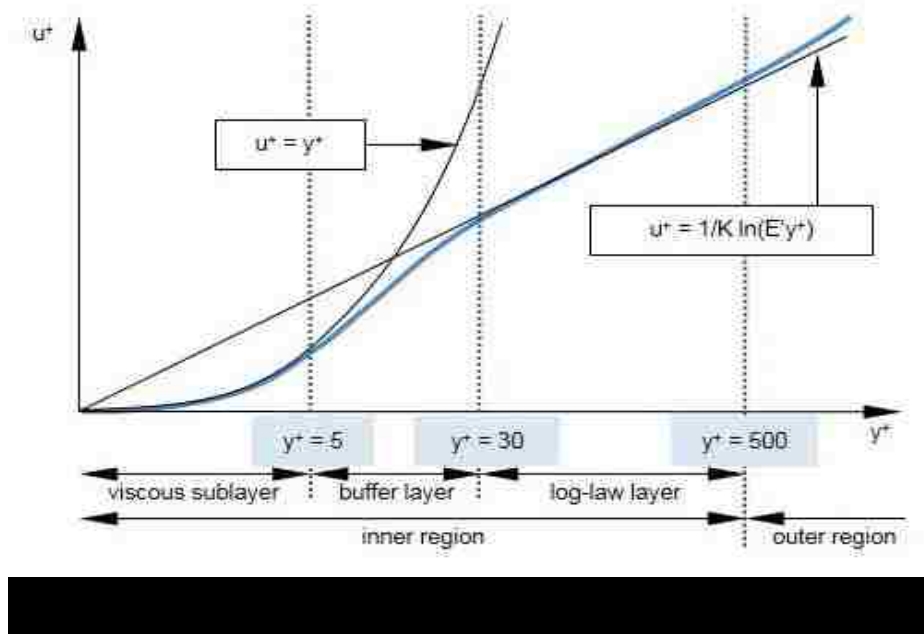
$E=9.8$

$B=5.5$

These values are for smooth walls, and wall roughness decreases the value of B. Note that K and B are universal constants for all turbulent flows past smooth walls at a high Reynolds number.

3. Buffer layer

This layer is a transitional layer between the above-mentioned layers.



2.2.2 Turbulence Modeling

To solve the behavior of the turbulent flow, it is necessary to use one of the common turbulence models. A turbulence model is a computational procedure to solve mean flow equations 2.6, 2.7, 2.8, 2.9 and 2.10. A turbulence model used in CFD code should be simple, accurate and economical to run. The most common turbulence models are represented in Table 2.2.

Table 2. 2. The Most Common Turbulence Models In CFD Simulation Software.

| | |
|-----------------------|---|
| Classical models | Based on Reynold equations: <ol style="list-style-type: none"> 1. Zero equation model- Mixing length model 2. Two-equation model- $k - \varepsilon$ model 3. Two- equation model- $k - \Omega$ model 4. Reynolds stress equation model 5. Algebraic stress model |
| Large eddy simulation | Based on space-filtered equations |

In classic models, the $k - \varepsilon$ is the most commonly used and validated model. It achieves very important results in calculating a wide variety of thin shear layer and recirculating flows without the needs for adjusting constants case by case. The $k - \varepsilon$ model works perfectly for flows in which the Reynolds shear stresses are most important. In other words, not only is $k - \varepsilon$ model the simplest turbulence model, which only needs boundary conditions to be supplied, but also it has an excellent performance for many industrially relevant flows and it is the most validated model for turbulence models.

However, the $k - \varepsilon$ model has been reported to not perform well for some unconfined flows, swirling and rotating flows and fully developed flows in non-circular ducts. In addition, it is more expensive to use than mixing length models.

The transport equations used for k and ε are as follows:

$$\frac{\partial(\rho k)}{\partial t} + \text{div}(\rho k U) = \text{div} \left[\frac{\mu_t}{\sigma_k} \text{grad } k \right] + 2\mu_t E_{ij} \cdot E_{ij} - \rho \varepsilon \quad (2.15)$$

$$\frac{\partial(\rho \varepsilon)}{\partial t} + \text{div}(\rho \varepsilon U) = \text{div} \left[\frac{\mu_t}{\sigma_\varepsilon} \text{grad } \varepsilon \right] + \frac{C_{1\varepsilon} \varepsilon}{k} 2\mu_t E_{ij} \cdot E_{ij} - \frac{C_{2\varepsilon} \rho \varepsilon^2}{k} \quad (2.16)$$

Where

$$\mu_t = \frac{\rho C_\mu k^2}{\varepsilon} \quad (2.17)$$

The first group of parameters mentioned in the above equations are the rate of change of k plus the second group of parameters, which are the transport of k or ε by convection. On the other side of the equations, the first set of parameters represents the transport of k or ε by diffusion, the second set are the rate of production of k or ε and the third set are the rate of destruction of k or ε .

There are five constants $C_\mu, \sigma_k, \sigma_\varepsilon, C_{1\varepsilon}, C_{2\varepsilon}$ in the above-mentioned equations with specific values, which fit for a wide range of turbulent flows:

$$C_\mu = 0.09; \sigma_k = 1; \sigma_\varepsilon = 1.3; C_{1\varepsilon} = 1.44; C_{2\varepsilon} = 1.92 \quad (2.18)$$

2.3 Final Remarks

This chapter provides a glimpse of the criteria needed to be considered in CFD simulation. The role of turbulence in CFD simulation is remarkable. Turbulence is a phenomenon with a great complexity and has puzzled theoreticians for over a hundred year. What makes it so difficult is the wide range of length and time scales of motion even in simple flows. Therefore, using a model compatible in expressing the main features of the wide range of turbulent flows is necessary. In this regard, the $k - \varepsilon$ model is highly recommended for general purpose CFD simulations. Moreover, Realizable Two-Layer K-Epsilon model gives good result on fine meshes which is used in the current study.

CHAPTER 3

CFD MODEL DESCRIPTION

3.1. 3D CAD Model

A 3D model is a solid model needed for CFD simulation. This model can be designed either by Computer-aided design software (such as SolidWorks, AutoCAD, CATIA) or CFD modeling software (such as FLUENT, STAR-CCM+) using the feature-based parametric solid modeling tools. In the current study, the CAD model has been designed by SolidWorks 2017 software and imported to STAR-CCM+ for CFD simulation purposes. Note that the model created by SolidWorks is compatible to run in STAR-CCM+, which is one of the most important features considered in SolidWorks. All details such as windows, doors, all internal and external walls, inlet and exhaust outlets have been designed in SolidWorks. Four models are created since four various strategies are considered for the location of outlets.

Generally, the models used in the current study to run CFD simulation are classified into three groups:

1. Flow Field Models: Equation of state and Fluid models
2. Heat Transfer Models: Solar load calculation and Heat transfer models
3. Grid Generation Model

3.2 Flow Field Models

3.2.1. Equation of State Model

For modeling the behavior of the air inside the building, it is necessary to define Equation of State model for the flow geometry. Using this equation, density and density derivative are

computed with respect to pressure and temperature. STAR-CCM+ offers different models such as Constant density, Ideal gas, Polynomial density, Real gas and Thermal non-equilibrium ideal gas, which can be used based on the features of the operation fluid. In the current study, Ideal gas model is used since we are dealing with air and using this model is needed to express density as a function of temperature and pressure.

3.2.2. Fluid Model

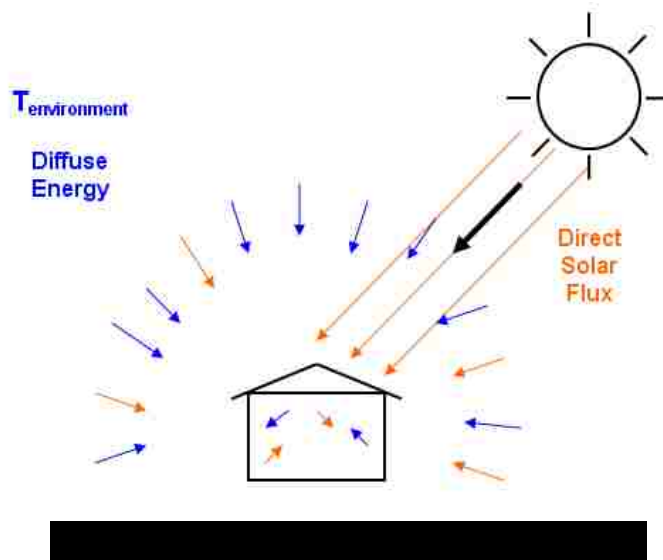
The indoor air is considered to contain 8 % humidity with the temperature of 42°C, which is the typical Las Vegas weather condition in summer. The inlet air from the evaporative cooler is 3000 cfm with the temperature of 22°C and 60 % relative humidity. Since this system contains a multi-component fluid mixture, it needs to consider a multi-component gas model, and a Non-reacting system as the constituents of air do not react chemically with each other.

In STAR-CCM+, different types of flow can be modeled such as Spalart- Allmaras, K-Epsilon, and K- Omega models. In the current study, the **Realizable Two- Layer K- Epsilon** model is considered, which contains a new transport equation for the turbulent dissipation rate ε and a critical coefficient of the model C_{μ} . C_{μ} is defined as a function of mean flow and turbulence properties.

3.3 Heat Transfer Models

3.3.1. Solar Load Calculation Model

The solar model is used to calculate the radiation loads (direct and diffuse fluxes) from the sun. This model is available by selecting radiation model as the Surface-to-Surface radiation model in STAR-CCM+, which makes it possible to simulate thermal radiation transfers between diffuse surfaces. The effects of radiation are calculated within the region of the simulation and also between the regions. Moreover, the radiation transfer with the surrounding environment can be calculated by using the Surface-to-Surface radiation model. The schematic model of radiation is represented as follows in Figure 3.1.

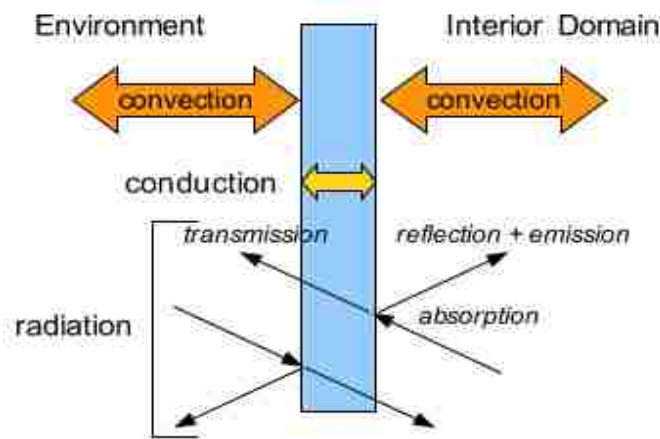


The radiation properties and the thermal boundary conditions on each surface should be set to define the amount of radiation that a surface receives and emits. In this regard, the surface properties such as temperature, emissivity, reflectivity, and transmissivity should be defined.

3.3.2. Heat Transfer Model

Regarding modeling the heat transfer of the current study, the Environment Boundary condition model is used for walls, external doors, windows, and roof. Using this boundary condition in STAR-CCM+ permits to calculate heat transfer terms simultaneously as follows:

1. Convection and radiation heat transfer between the external sides of flow geometry and the environment. The external surfaces can absorb, emit, reflect, and transmit radiation.
2. Heat conduction through the walls using the thermal resistance of walls structure
3. Heat convection and radiation from the internal side of the boundary into the internal domain

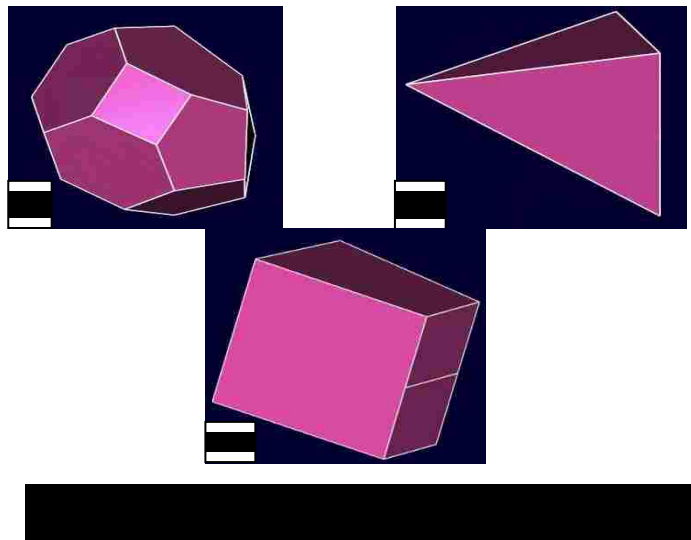


3.4. Grid Generation

The basis of all simulation software in CFD studies is the mesh, which is also called grid. Typically, the first step before beginning CFD simulation to get results is creating a mesh for the model. Therefore, meshing is one of the critical aspects in the CFD process and without a good understanding of its structure we cannot expect any desired result from the CFD simulation. In other word, the accuracy of CFD simulation results is directly linked to the meshing, which

means the better meshing brings results with more accuracy. Basically, a mesh is needed since variables like flow behavior such as velocity, pressure and temperature and also heat transfer should be solved for each part of the model. Therefore, meshing, which creates a huge number of cells, is needed to solve all these variables for each cell.

Appropriate shape and size of each cell are one of the most important aspects in obtaining accurate results. First, course meshing will be considered for the model. Then, the result will be analyzed with the results obtained from the refined grids. In another word, the simulation will be done with different based size and growth rate and then the mesh will be refined. This process will be continued until slight changes are observed in the results to ensure mesh independency of the results.



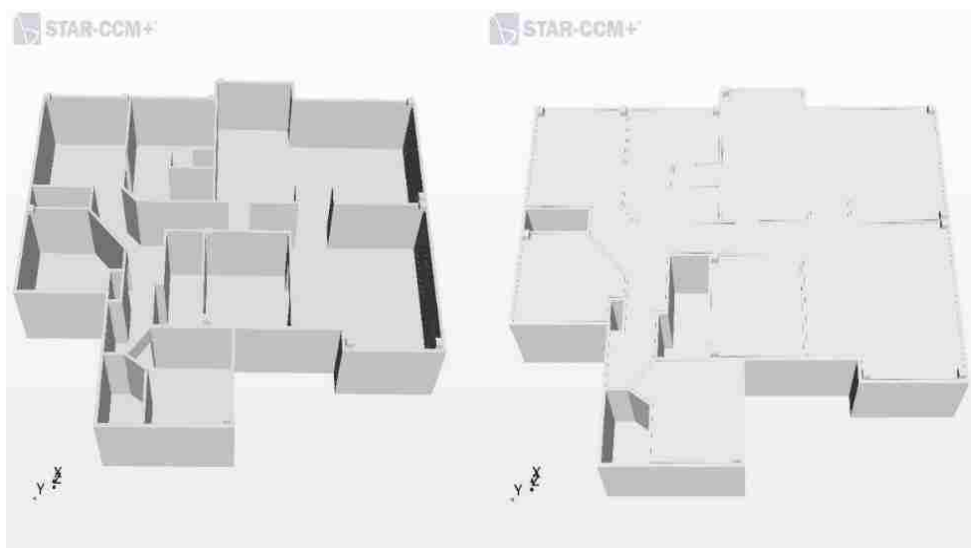
STAR-CCM+ provides different meshers and tools to generate a suitable mesh for various geometries. There are different kinds of meshers such as Surface Wrapper, Surface Remesher, Polyhedral, Tetrahedral and Trimmed meshers, which are the most common meshers, and have been represented in Figure 3.3.

In the current study, 2 mesh operations are used to simulate the flow inside the model:

1. Surface Wrapper
2. Automated Mesh

3.4.1. Surface Wrapper

In complex models, there may occur some errors while we are trying to mesh the model. The problem is the complexity of the imported model along with incompatibilities between the CAD model software and STAR-CCM+. Therefore, the model cannot be performed as an integrated model and an automatic mesh through all parts of the body is impossible. Moreover, since we are going to model fluid, we need to collect all fluid (in the current study, air) inside the model and there is no need to model solid structure. Catching all fluid region inside a complex model is difficult and time-consuming. A solution to this problem is a feature called Surface wrapper in STAR-CCM+, which allows us to acquire all fluid inside the body as an integrated model (Figure 3.4).



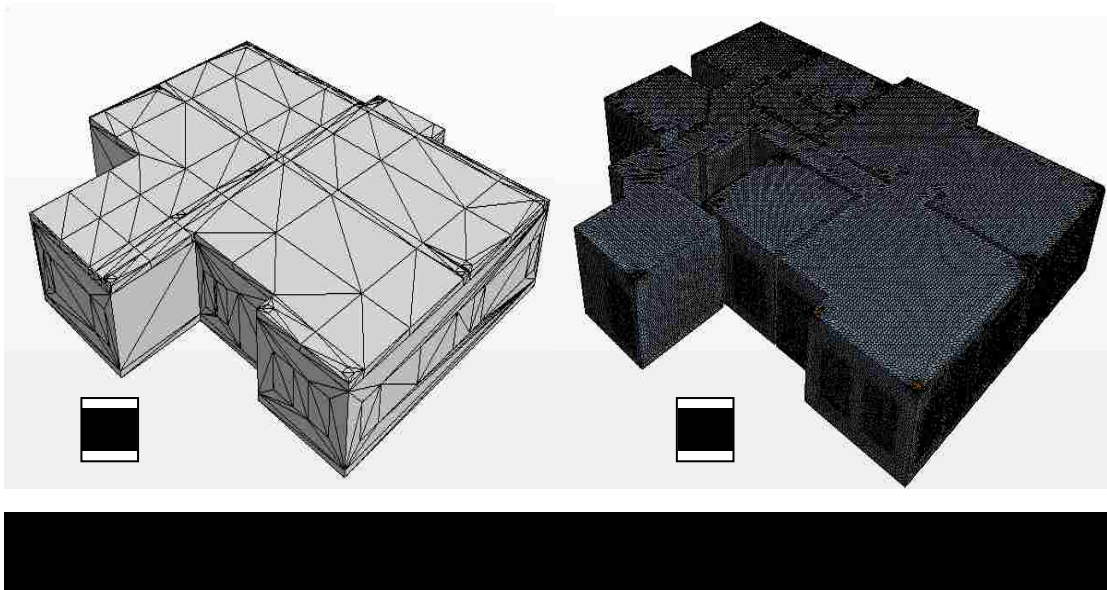
3.4.2 Automated Mesh

The Automated mesh operation is used to generate surface and volumes meshes for its input parts. It manages all of the mesher, default controls and custom controls. To refine the automated mesh operation, 3 meshers are used as follows:

- Surface Remesher
- Polyhedral Remesher (Core Volume Mesher)
- Prism Layer Remesher (Core Volume Mesher)

3.4.2.1 Surface Remesher

The surface remesher is used to retriangulate the surface in order to improve the quality of the surface and optimize it for the volume mesh models. The remeshing is based on a targeted edge length and include feature refinement based on curvature and surface proximity. Localized refinement for boundaries and near-wall surfaces can also be included. An example is represented in Figure 3.5 including starting surface and the remeshed surface.



3.4.2.2 Polyhedral Mesher

As mentioned, different models are available for volume meshing such as Tetrahedral, Polyhedral and trimmed mesher. In the current study, the polyhedral mesh model is used since this model provides higher accuracy in complex mesh generation problems. The polyhedral mesh has been derived directly from tetrahedral mesh by forming polygon around each node of tetrahedral mesh. Therefore, the number of mesh cells are lower in polyhedral mesh in comparison with the tetrahedral and trimmed methods. Some of the advantages of polyhedral mesh, which is used in the current study, are as follows:

- Faster convergence with fewer iterations
- Lower volume in comparison with other methods
- Lower residual value in convergence
- Faster runtimes than other methods.

3.4.2.3 Prism Layer Mesher

Prism Layer Mesher model is used with a core volume mesh to generate orthogonal prismatic cells next to the wall surface and boundaries. In order to improve the accuracy of the flow solution, using this layer of cells is necessary. Prism layer allows solver to resolve near-wall flow more accurately. Defining the flow distribution near the walls is critical not only on the heat transfer and Buoyancy forces, but also flow features such as separation. Separation affects the final results including drag and pressure drop. Regarding getting an accurate prediction of flow features, it's necessary to resolve the velocity and temperature gradients normal to the wall. These gradients are much steeper in the viscous sublayer of a turbulent boundary layer and using a prism layer mesh allows us to resolve the viscous sublayer directly.

Moreover, prism layers reduce numerical diffusion near the wall. Numerical diffusion is a discretization error, which causes discontinuities and steep gradients in a finite volume model. When the fluid is aligned with the mesh, the numerical diffusion is minimized. In this regard, the use of prism layer enhances accuracy.

A prism layer is defined based on its thickness, the number of cell layers, the size distribution of the layers and the function that is used to define the distribution. An example volume mesh showing five prism layers next to the wall surface is shown below in Figure 3.6.

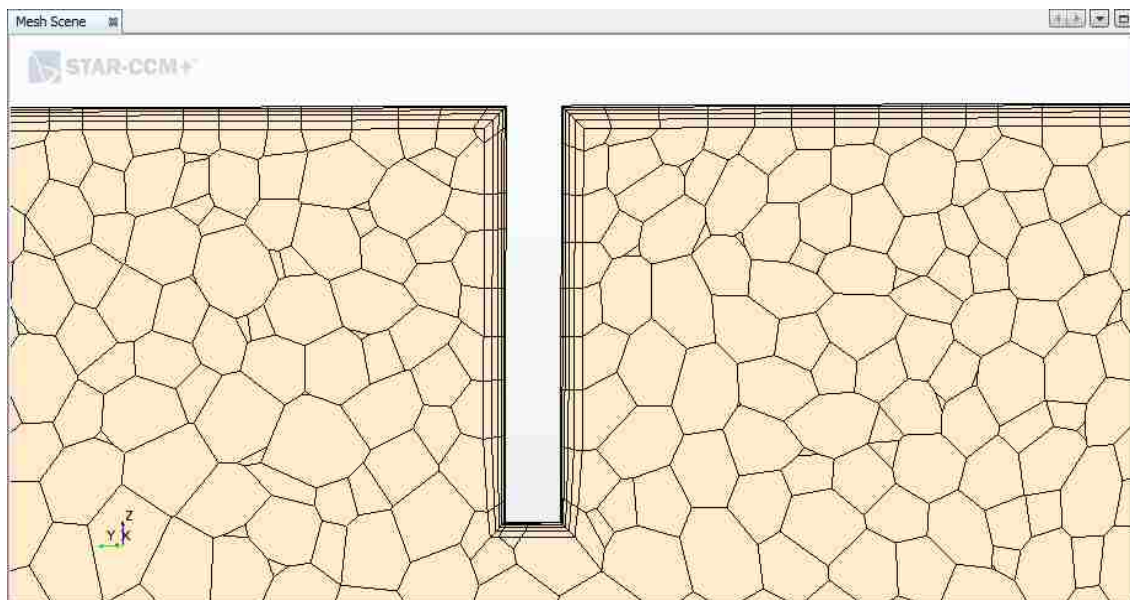


Figure 3. 6 Volume Mesh With 5 Prism Layers

CHAPTER 4

PROBLEM DEFINITION AND BOUNDARY CONDITIONS

4.1 Problem Description

The intended model is a typical house in Las Vegas (Figure 4.1, 4.2, 4.3), assuming the floor to be in contact with the ground and with the walls and roof in contact with the ambient environment. It is assumed that the house has an unventilated attic and has been equipped with an evaporative cooler connected from the door of the garage.

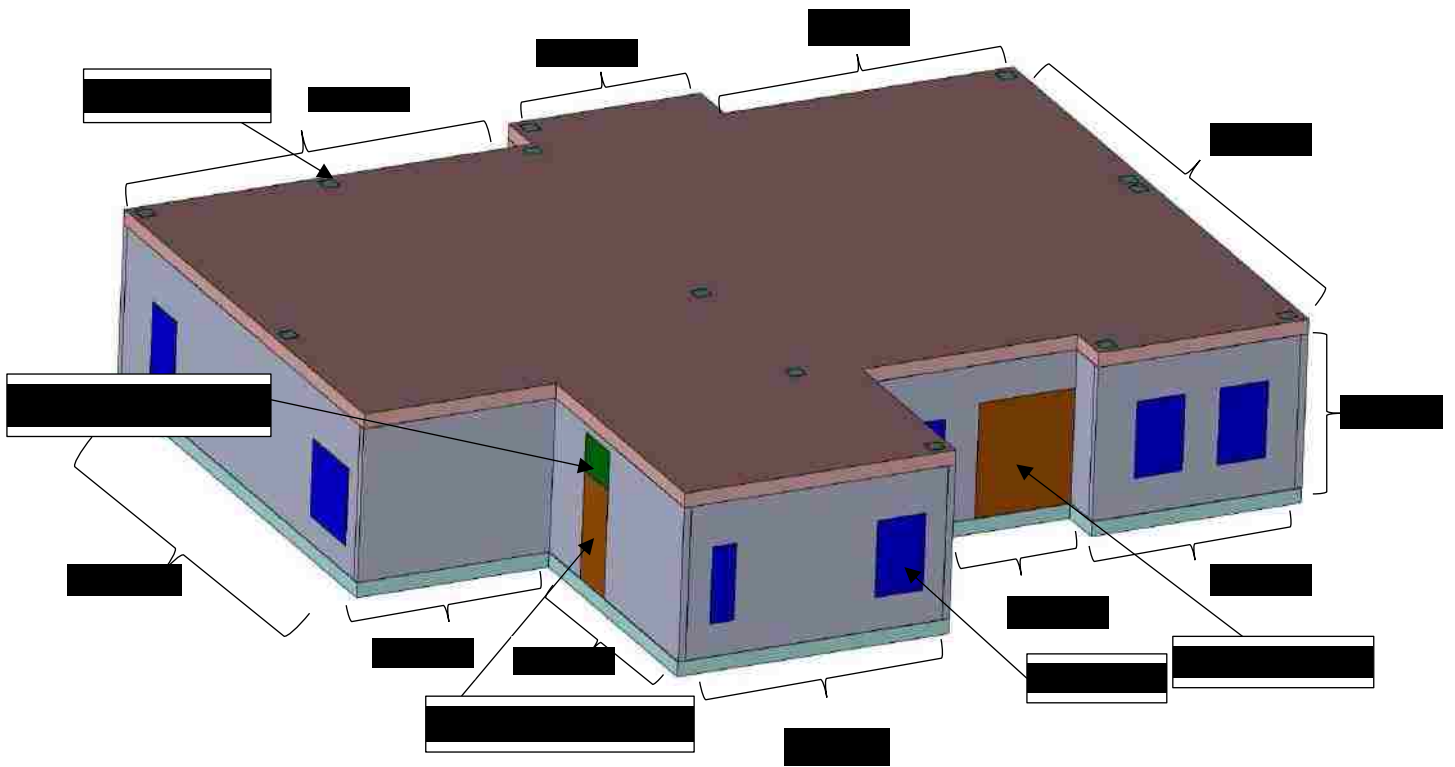
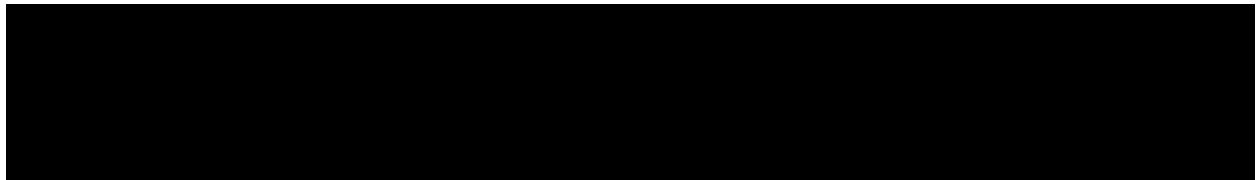
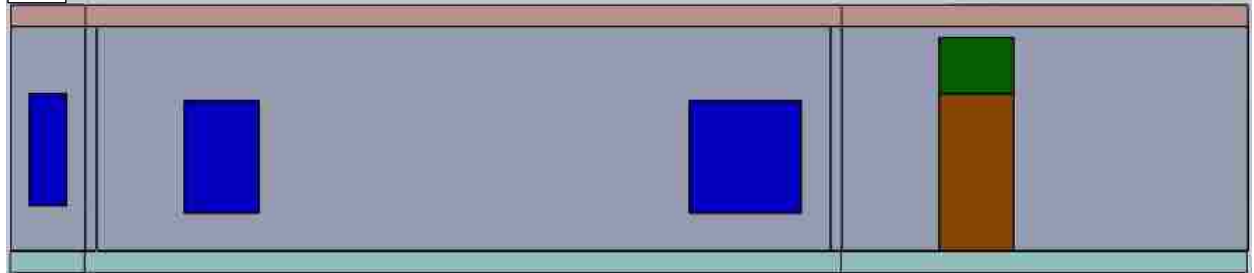
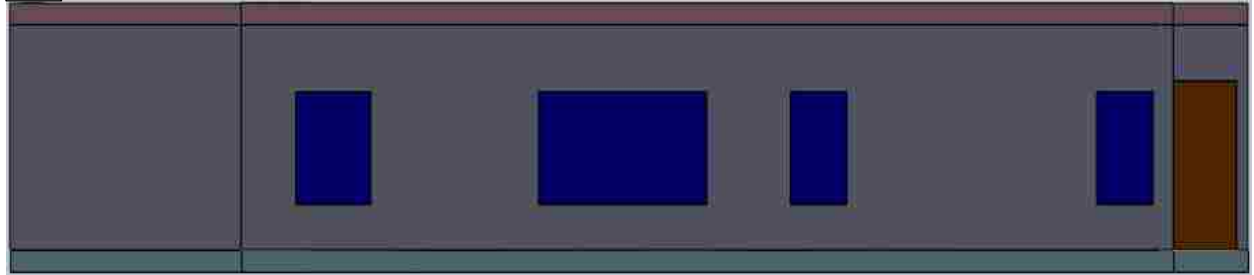
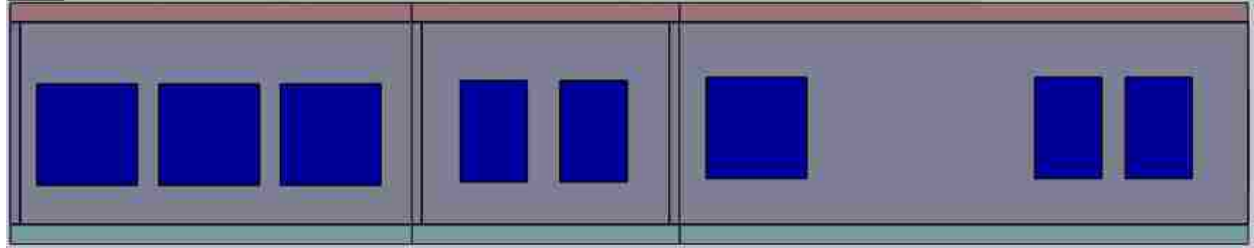
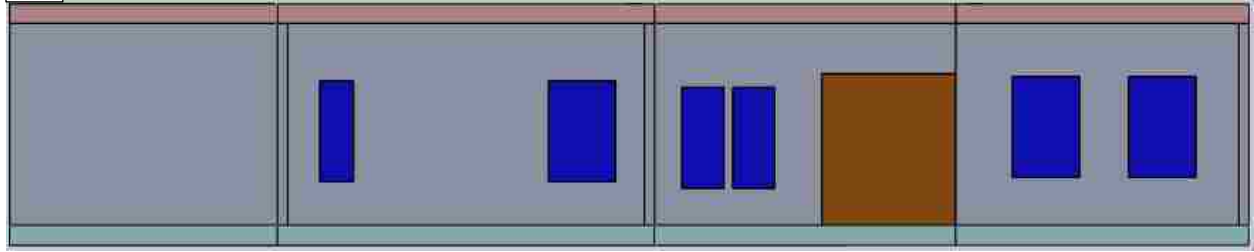
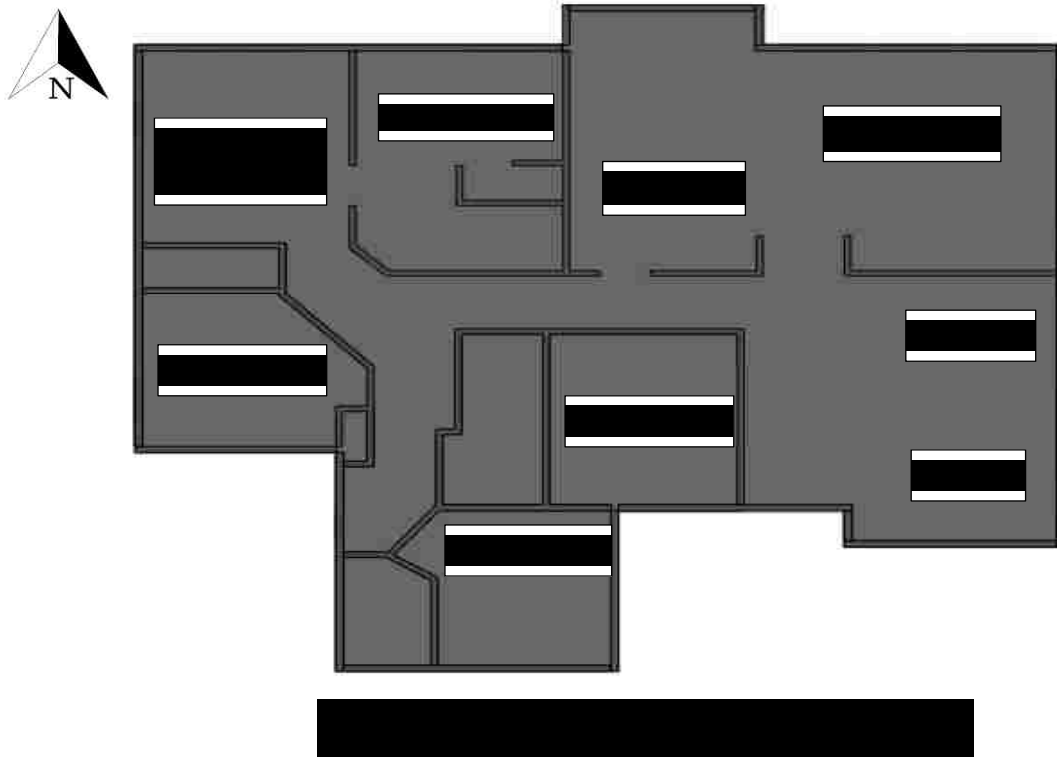


Figure 4. 1 Flow Geometry and Solution Field (Perspective View)





As it has been shown in Figure 4.1, the evaporative cooler (The green rectangle) has been connected from the top of the door of the garage and there are 13 ceiling vents in different sections of the house. Note that, the attic, the roof, and the garage have not been included in the flow geometry since they are assumed to be as the unventilated spaces.

The ventilation occurs based on the pressure difference between the evaporative cooler inlet and 13 ceiling vents, which causes free cold air to move into each room to maintain temperature and humidity based on the thermal comfort standards.

The relative humidity will be different at each point of the geometry since the percentage of relative humidity will change as it will be warmed by gaining heat from the inside air because a portion of the humidity will be evaporated due to absorption of the heat. The heat and excess

humidity will be removed from the rooms by exhaust ventilation due to the pressure difference between the inlet air from the evaporative cooler and the located exhaust vents in each room.

In the current study, four various strategies are considered for the Exhaust Vent's locations in the ceiling (Stack Ventilation), and the goal is to examine how various locations can increase the energy efficiency and facilitation to approach the desired thermal comfort inside the house. As it is represented in Figure 4.4, outlet strategies are as follows:

- A. The longest distance from the door in each room (The geometry mentioned in Figure 4.1 belongs to this strategy)
- B. Outlets are in the center of each room. For rooms with more than 1 outlet, all outlets are adjoined to each other in the center of each room
- C. Outlets are in the center of each room. For rooms with more than 1 outlet, the outlets are located in the center of rooms with equal distance from each other and the adjacent wall.
- D. Outlets are located on the intersection of the ceiling and the middle of the walls.



Four strategies are evaluated in three different hours on July 23, which is the hottest day in Las Vegas. The hours are 12 p.m., 3 p.m. and 5 p.m. The results will be presented in chapter 5 and the strategies will be evaluated based on the thermal comfort standards (presenting temperature profile, humidity profiles and tabulated thermal comfort data evaluation), Pressure profile, Density profile and Specific heat in the critical sections of the house. The most critical parts are the closest sections to the inlet (Bedroom 1 & 2) and the farthest section from the inlet (Bedroom 3). General results of all sections of the house will be represented as well to evaluate the average condition maintained in the house to clarify, which strategy would be the most appropriate.

4.2 Surface Boundary Conditions

4.2.1 Ambient Environment Condition

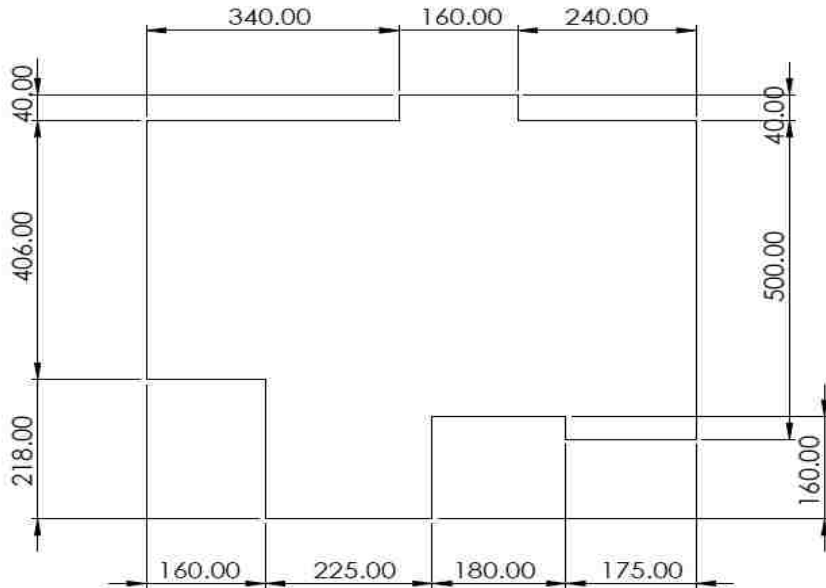
The ambient dry bulb temperature is assumed to be 42°C (108°F), the wet bulb temperature 19°C (66°F) and the relative humidity of 8 %. The garage is separated from the internal environment with two walls and one door. These walls and door are assumed to be in the constant temperature of 40 °C (104°F) since the garage is an unventilated space.

4.2.2 Dimension Details

The building details including height, the area of the ventilated space and windows details are represented in Table 4.1 and Figure 4.5.

Table 4. 1. Building General Details.

| Details | Dimension (IPS) | Dimension (SI) |
|--|---------------------------|-----------------------------------|
| Evaporative Cooler Inlet | 40×30 inch ² | 1.016×0.762 m ² |
| Exhaust Air Vent | 12×12 inch ² | 0.3048×0.3048 m ² |
| Windows | 20×60×6 inch ³ | 0.508×1.524×0.1524 m ³ |
| | 25×60×6 inch ³ | 0.635×1.524×0.1524 m ³ |
| | 30×60×6 inch ³ | 0.762×1.524×0.1524 m ³ |
| | 40×60×6 inch ³ | 1.016×1.524×0.1524 m ³ |
| | 60×60×6 inch ³ | 1.524×1.524×0.1524 m ³ |
| Height of External doors | 90×60×6 inch ³ | 2.286×1.524×0.1524 m ³ |
| | 40×90×6 inch ³ | 1.016×1.524×0.1524 m ³ |
| | 80×90×6 inch ³ | 2.032×1.524×0.1524 m ³ |
| Area (without garage) –Ventilated space | 2660 ft ² | 247.12 m ² |
| Height of the Building | 120 inch | 3.048 m |



4.2.3 Materials Properties

The materials used in the walls, roof, windows, and doors are represented as follows in

Table 4.2-4.4.

Table 4. 2. Details Of The External Walls.

| Materials | R (hr-ft ² -F/BTU) | R [m ² K/W] | Comment |
|---------------------------------------|-------------------------------|------------------------|--|
| 1 Inch Stucco | 0.19984 | 0.0352 | - |
| 0.5 inch OSB | 0.62 | 0.11 | - |
| Wood Stud Nominal 2*4 | 4.38 (U=0.2283) | 1.296 | Assume the insulation cavity occupies approximately 91 % of the area and studs occupy 9% so: U=0.91×0.059+0.09×0.2283=0.074 Btu/hr-ft ² -F [0.3254 W/m ² K] |
| Fiber Batt Insulation | 17 (U=0.059) | 2.985 | |
| 0.5 inch dry wall (gypsum wall board) | 0.45 | 0.08 | - |
| R total | 14.7402 | 2.596 | - |
| Total Thickness | inch | cm | - |
| | 4+0.5+0.5+1=6 | 15.24 | |

Table 4. 3. Details Of The External Doors And Windows.

| External Doors | | | Windows | | |
|---|------------------------------|------------------------|--|------------------------------|-----------------------|
| Materials | R (hr-ft ² F/BTU) | R [m ² K/W] | Materials | U(Btu/hr-ft ² -F) | U[W/m ² K] |
| Wood door with 1 $\frac{3}{4}$ inch thickness, solid core (No storm door) | 3.125 | 0.55 | ½ inch air space – e=0.2/ Double glass | 0.3 | [1.7] |
| | | | Wood Frame (Factor 0.95-1) | - | - |
| | | | U total | 0.95×0.3 | 0.95×1.7 |

Table 4. 4. Details Of The Roof And Ceiling.

| Roof | | | Ceiling | | |
|---------------|------------------------------|-----------------------|------------------------|-------------------------------|------------------------|
| Materials | U(Btu/hr-ft ² -F) | U[W/m ² K] | Materials | R (hr-ft ² -F/BTU) | R [m ² K/W] |
| Wood Shingles | 0.53 | 3 | 0.5 inch Dry Wall | 0.45 | 0.079 |
| | | | 9 inch Fiberglass batt | 9*3.8 | 0.67 |
| | | | R total | 34.65 | |

All external walls have been assumed to be in contact with the outside and the heat is assumed to be transferred in terms of radiation, convection, and conduction through the walls. The surface emissivity has been assumed to be 0.9 for walls, 0.885 for doors and 0.95 for windows.

4.2.4 Roof and Ceiling Properties

Since the ceiling has been connected to the attic, it is necessary to calculate the temperature of the attic in order to calculate cooling load regarding to provide thermal comfort inside the house. In this regard, the air temperature of the attic can be calculated using the below formula:

$$T_{attic} = \frac{T_i(A_1U_1) + T_0(A_0U_0)}{A_1U_1 + A_0U_0} \quad (4.1)$$

Where

A₁= Ceiling area

U₁= Heat transfer coefficient of the ceiling

A₀= Roof area: assume is 1.6 times of the Ceiling area

U₀= Heat transfer coefficient of the roof

T_i= Air temperature just below the ceiling

T₀= Environment Temperature

Therefore, T_{attic}=107.14 F (41.74°C).

Since we assumed constant heat flux boundary condition for the ceiling, we need to calculate the heat flux using the below formula:

$$Q = U_1A_1(T_{attic} - T_i) \quad (4.2)$$

Since it has been assumed that the attic is an unventilated space, the average heat flux should be added to this boundary based on the maximum acceptable air temperature. The maximum indoor temperature acceptable based on the ASHRAE Standard 55 for providing thermal comfort should not exceed from 28 °C (82.4°F). Therefore, we set the maximum acceptable temperature just below the ceiling as T_i=82.4°F.

4.2.5 Inlet Condition

As it is represented in section 1.2.3, which is dedicated to the evaporative cooling calculation, the inlet air boundary condition will be calculated based on the ambient wet bulb

temperature, dry bulb temperature, and relative humidity. The efficiency of an evaporative cooler can be calculated as follow:

$$\varepsilon = \frac{T_{i,db} - T_{e,db}}{T_{i,db} - T_{i,wb}} \quad (4.3)$$

Where:

ε : is the efficiency of an evaporative cooler. For a direct evaporative cooler, the efficiency is assumed to be 85 %.

$T_{i,db}$: is the dry bulb temperature of the ambient air, which is entered to the evaporative cooler. For the current study, it is assumed to be equal to 42°C .

$T_{i,wb}$: is the wet bulb temperature of the ambient air, which is entered to the evaporative cooler. As it is described in Figure 1.2, using the psychrometric chart, the wet bulb temperature is equal to 19°C for the current study

$T_{e,db}$: is the moist air temperature at the exit, which is the ventilated air entered from inlet into the internal environment

From the above-mentioned equation, the inlet ventilated air can be calculated, which is equal to 22.45 °C (72.41°F). Using the psychrometric chart, the relative humidity of the air at the inlet can be concluded as 60 %.

The cooling load of the house has been calculated by Carrier HAP software. Based on all the details such as wall and window properties and ambient condition for Las Vegas on July 23, the minimum needed volumetric flow rate for this house is considered to be 3000 CFM.

Therefore, the velocity can be determined at the inlet as follows:

$$V = \frac{Q}{A} \quad (4.4)$$

Where:

Q : Volumetric flow rate (CFM)

A : Area of the inlet (8.33 ft²)

Therefore:

$$V = \frac{3000}{8.33} = 6.0024 \text{ ft/s}$$

To clarify that there is a turbulent flow at the inlet, the Reynolds number must be calculated. If the Reynolds number is higher than 2500, it means that we have a turbulent flow at the inlet. The Reynolds number can be calculated as follow:

$$Re = \frac{\rho u D_H}{\mu}$$

Where:

u : Velocity at the inlet

D_H : Equivalent Diameter of the inlet = 2.85 ft (0.86)

ρ : Density of moist air at the inlet = $1.186 \frac{Kg}{m^3}$

μ : Dynamic viscosity of the moist air = $1.06 \times 10^{-5} \frac{Kg}{m.s}$

Therefore, the Reynolds number is equal to 1.76×10^5 , which means we have a turbulent flow at the inlet. To summarize, the boundary condition at the inlet will be defined as:

1. Velocity Inlet Boundary model
2. Temperature is set to 22.45 °C (72.41°F)
3. Mass fraction is defined based on the relative humidity at the inlet, which is 60 %
4. The velocity is set as 6.0024 ft/s (1.83 m/s)

4.2.6 Exhaust Air Vents Condition

The outlet will be set as a Pressure Outlet model since the outlets are defined based on the pressure difference we considered for this study. The exit gauge pressure is assumed to be 0 since typically the atmospheric pressure is defined at the outlet of buildings in normal condition.

One of the most important parts of this study is dedicated to the mass conservation aspect. In another word, the solution is only acceptable when all the intake air from the Inlet will be exited from the outlets. In this regard, the total mass flow rate in the outlets should be equal to the mass flow rate at the inlet. Addressing this concern, the mass flow rate at the inlet can be calculated as follows:

$$\dot{m} = \rho AV = \rho Q \quad (4.5)$$

Where:

V : Velocity at the inlet

A : Inlet surface area=2.85 ft

ρ : Density of moist air at the inlet = $1.186 \frac{Kg}{m^3}$

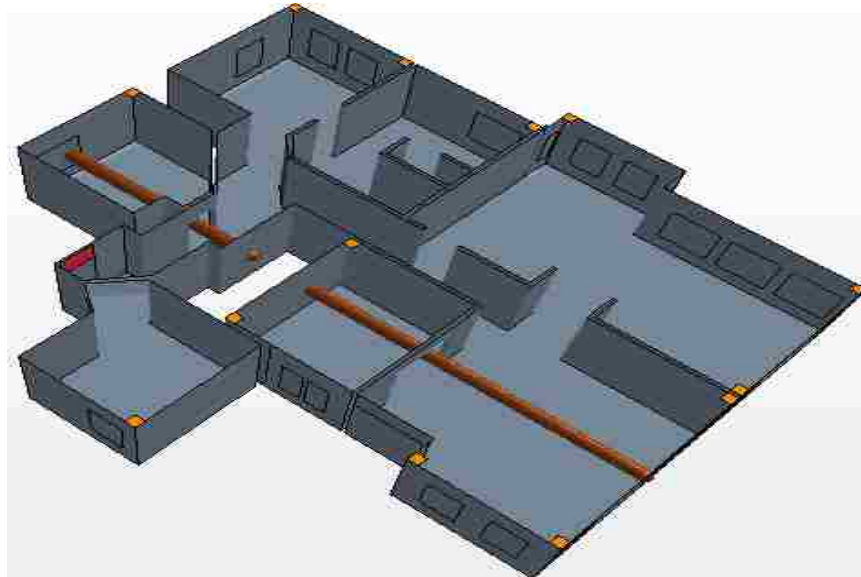
Using the mentioned values of volumetric flow rate and density, the mass flow rate at the inlet is equal to $1.679Kg/s$ and the total mass flow rate at the outlets should be verified with this value, which will be evaluated in Chapter 6 in detail.

CHAPTER 5

RESULTS AND DISCUSSION

5.1 Grid Independence Study

Grid independence study is one of the most important issues in numerical solutions. Grid Independence means that the results should be independent of the mesh resolution. In the current study, grid independency has been evaluated in terms of velocity and temperature profiles along an arbitrary line through all different sections of the model. In this regard, a line with the resolution of 200 is created, which temperature and velocity are evaluated along.



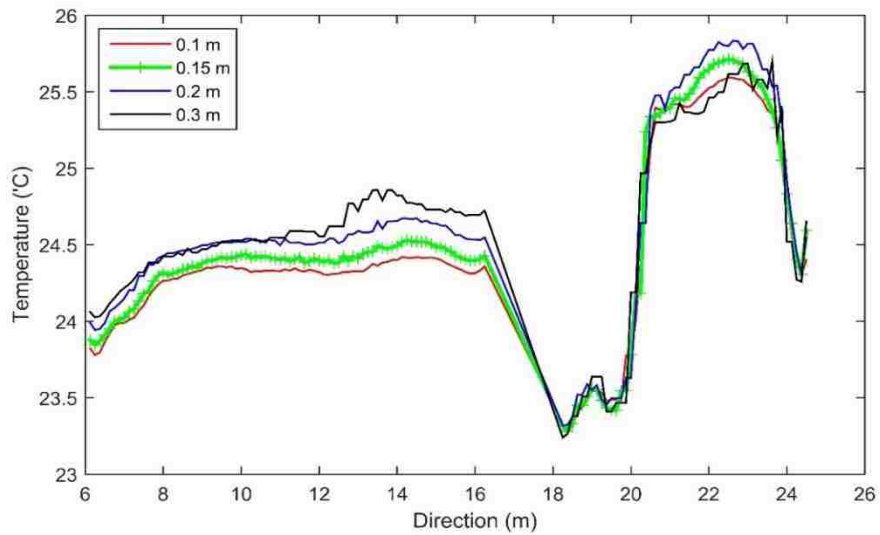
The process is to study changes in the temperature and velocity results in respect to variable mesh densities in order to provide a desired numerical accuracy in an optimum computational time. Different mesh densities are generated and solved in STAR-CCM+, and the result are presented in Table 5.1. The grid generation started from coarser mesh and then is refined to thinner densities. As the changes in temperature and velocity become smaller, the

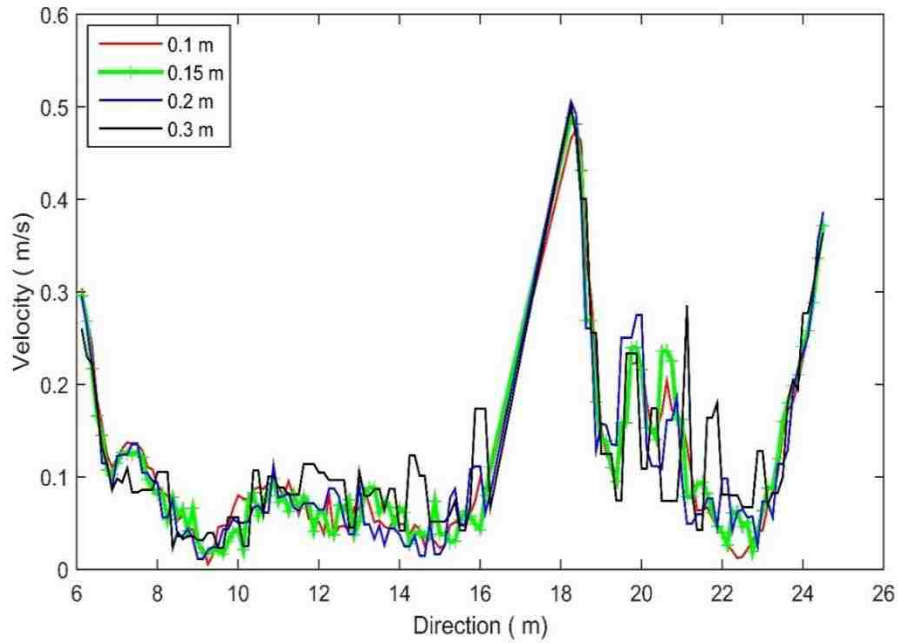
accuracy of the numerical results will be increased, and by approaching a negligible difference between different meshes the final grid density can be selected. This means the solution is independent from the number of cells in the chosen mesh grid.

Table 5. 1. Mesh Properties Used for Grid Independency.

| No | Base Size (m) | Number of Prism Layers (33 % of Base size) | Number of Cells |
|----|---------------|--|-----------------|
| 1 | 0.3 | 5 | 233,283 |
| 2 | 0.2 | 5 | 504,616 |
| 3 | 0.15 | 5 | 1,106,431 |
| 4 | 0.1 | 5 | 2,565,516 |

As presented in Figure 5.2 and Figure 5.3, it is obvious that the temperature and velocity profiles for base size 0.15 and 0.1 m are close and differences are negligible (Discrepancy less than 2 %). Therefore, we can conclude that the mesh grid with 0.15 m base size would be the desired grid to have independent results in an optimum computational time.



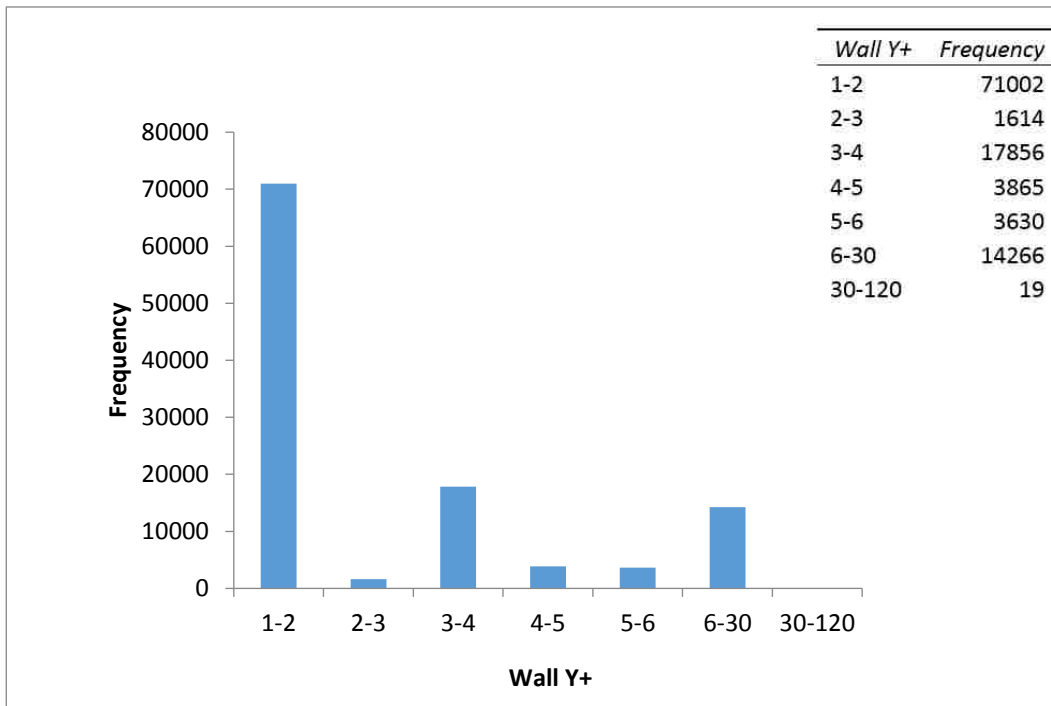
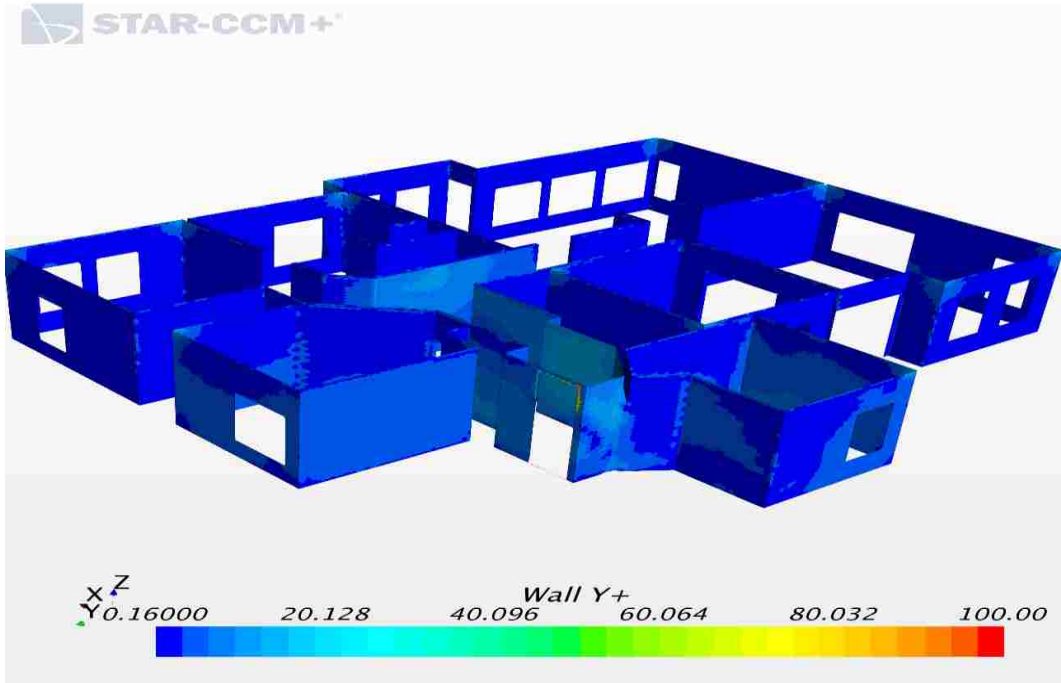


5.2 Wall Treatment Y^+

The final step for evaluating the mesh is Wall Treatment Analysis. The value of Y^+ should be less than 5 to make sure that viscous effects are considered in the simulation since the mean flow velocity depends on the fluid density, viscosity, distance from the wall and wall shear stress. Therefore, it is necessary to make sure that the mesh grid is fine enough near the walls to examine all effects there and as it has been mentioned in section 2.2.1, the mesh nodes should be located in the viscous sublayer ($Y^+ < 5$) to make sure the simulation results are accurate.

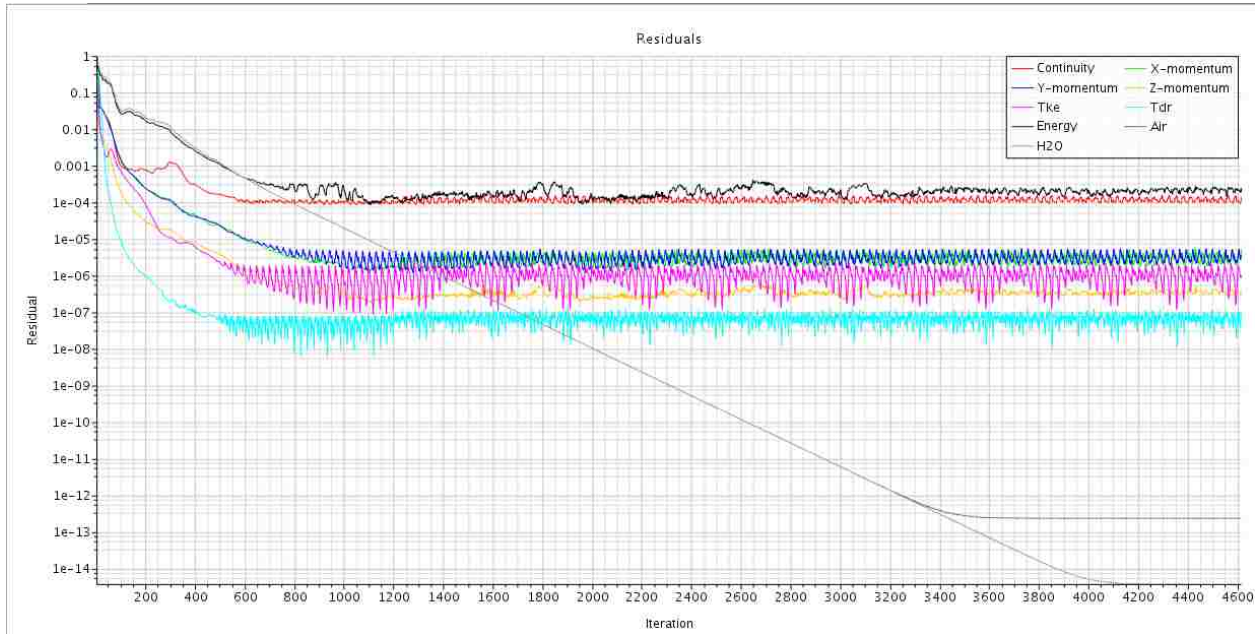
As it is represented in Figure 6.4 and Figure 5.5, the Y^+ value is mainly less than 5, which means the viscous sublayer is included in the simulation and the nodes are fine enough to evaluate flow behavior near the walls. However, it can be observed that some parts are in the buffer layer and some nodes are in the log layer regions although we have a fine mesh. These parts are located at the **Inlet of the evaporative cooler** and **Exhaust air vents** (Outlets). The

reason is that the flow is not fully developed at the inlet and the outlets and because of that, we will face a huge fluctuation in these regions. However, this situation cannot affect the results since they are at the entrance and the exit location of the study field.



5.3 Residual

As it is presented in Figure 6.6, the simulation is converged after 4300 iterations and residual for the air and water distributions in the model are $1e-11$ and $1e-13$, which certify the high accuracy of the numerical solution of the current study.



5.4 Validation of Results

In this study, we obtain the temperature and humidity profile in different sections of the house using STAR-CCM+ for various strategies of outlets. The problem is solved by considering the ambient environment and the solar radiation, ambient heat convection, conduction through the walls and heat convection inside the house, which are computed simultaneously. However, the papers published in this field mainly have investigated the temperature profile inside a building or humidity is only tracked in respect to different strategies for inlets with different temperature and relative humidity at the inlet [23]. The current study is validated by reference

[26] in terms of the mean temperature inside a 3×3×3 m room with a constant temperature boundary condition in the walls. The various conditions have been evaluated using mineral micro particle coating in the structure of the walls, conserve energy in the building by decreasing solar radiation absorption using this kind of coating.

According to the results presented in Table 5.2, the maximum discrepancy is about 0.04 %, which is acceptable and shows that the method used in the current study is accurate enough to regenerate previous works in the energy conservation field.

Table 5. 2 Mean Temperature (K) In The Middle Of The Room- The Result Of The Present Work And Reference [26].

| | No Coating (K) | mineral coating in both sides (K) | mineral coating on the internal side (K) | mineral coating on the external side (K) |
|----------------|-------------------|--------------------------------------|--|--|
| Reference [37] | 295.6 | 294.2 | 294.8 | 294.6 |
| Present Work | 295.61 | 294.22 | 294.68 | 294.5 |

5.5 Mass Conservation

The first step in evaluating the final results is obtaining the mass conservation. Based on the mass conservation law, the mass in a closed system should remain constant since the mass cannot be created or destroyed. As mentioned in section 5.2.6, the quantity of the mass entering the building from the inlet should be equivalent to the total amount of mass flow exiting from the vents (outlets) in the ceiling. As it is represented in Table 5.3, the mass conservation is evaluated in all of four strategies assumed in the current study.

Table 5. 3 Mass Conservation Of Current Study.

| Strategy | Mass flow in the Inlet (Kg/s) | Total Mass flow in 13 Outlets (Kg/s) |
|----------|-------------------------------|--------------------------------------|
| A | -1.67 | +1.67 |
| B | -1.67 | +1.67 |
| C | -1.67 | +1.67 |
| D | -1.67 | +1.67 |

5.6 Temperature in Different Strategies

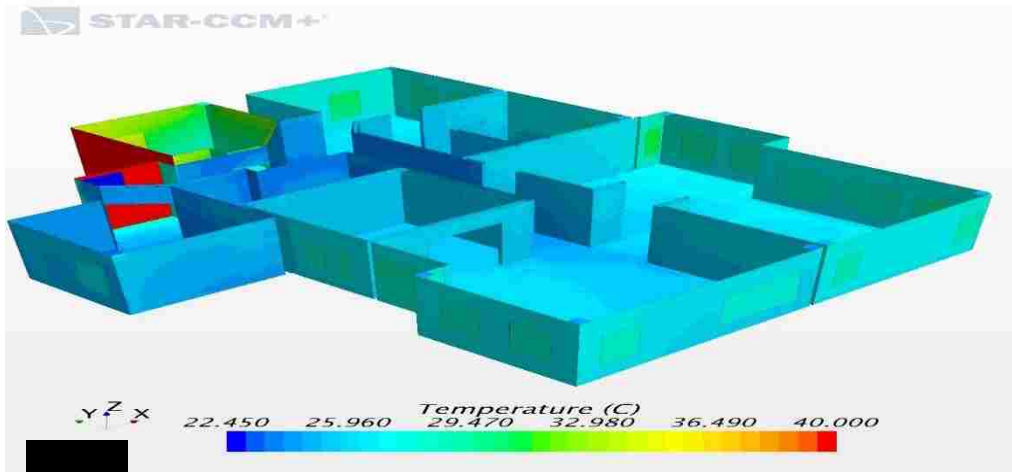
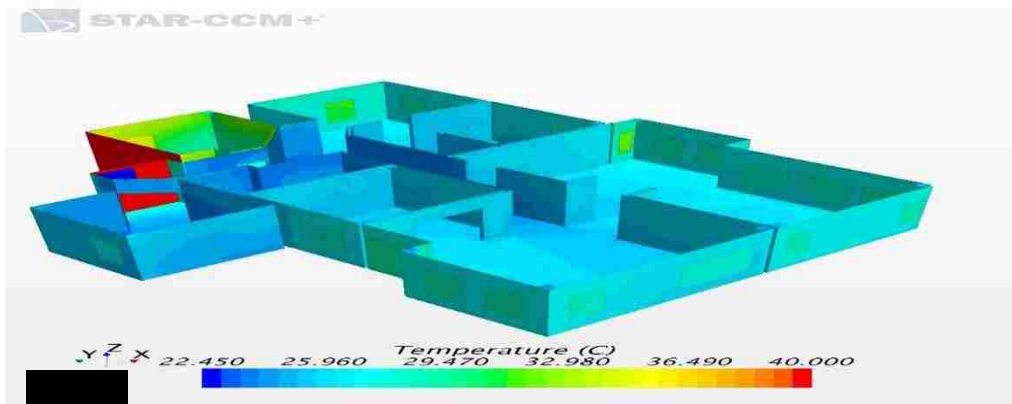
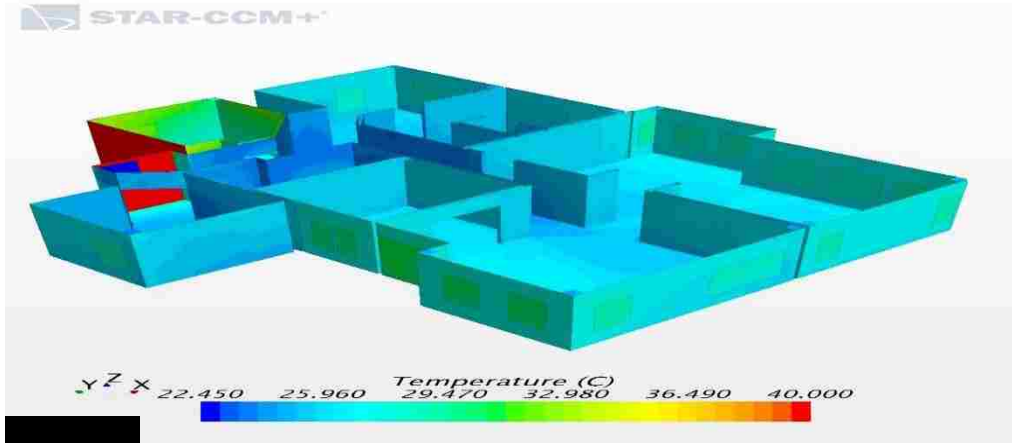
In the first step, Temperature profiles have been evaluated in the different sections of the house and the results are evaluated in the different strategies. The simulations are examined for three different hours (12, 3 and 5 p.m.) in each strategy and temperature profiles are evaluated in two different sections and a general view of temperature distribution is represented as well.

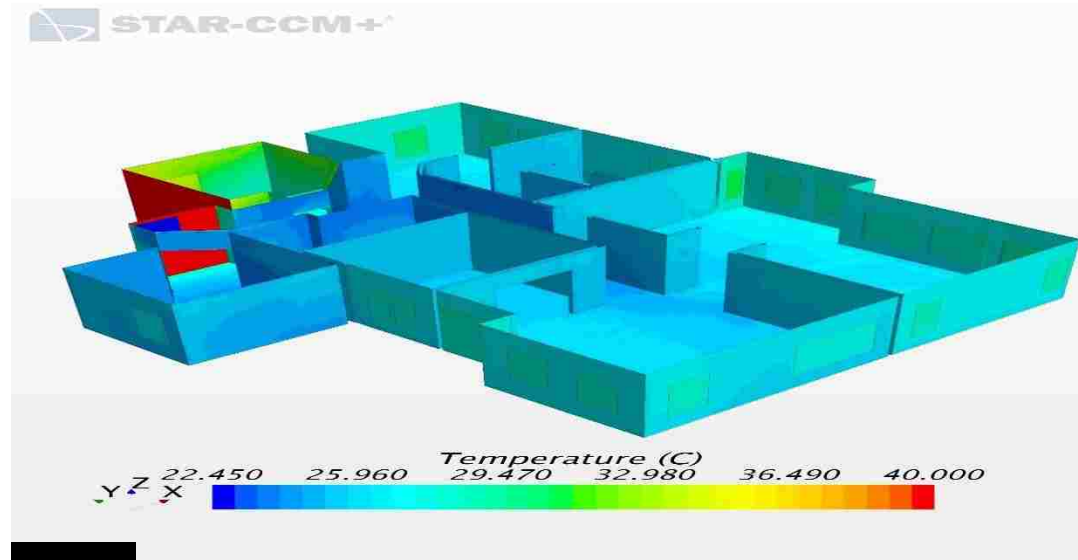
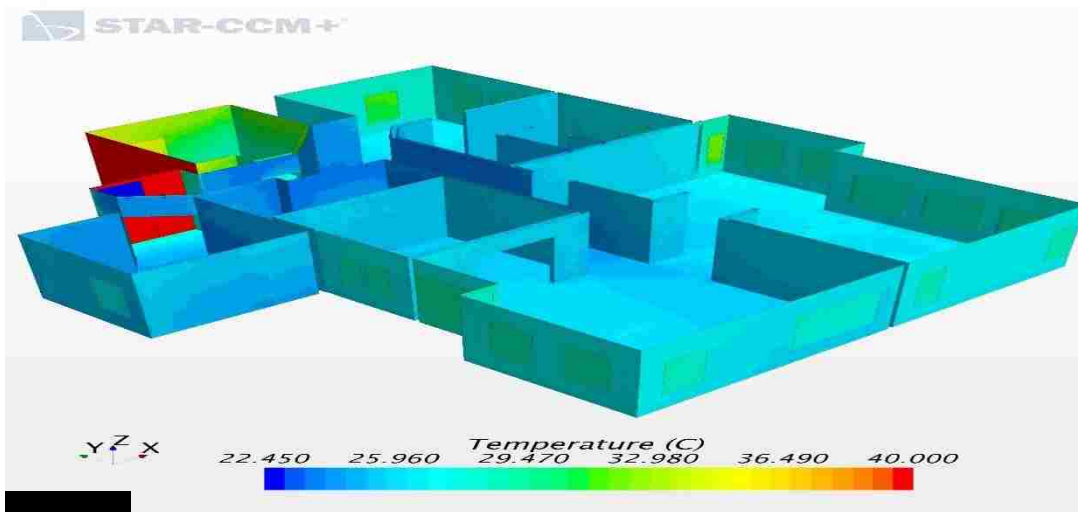
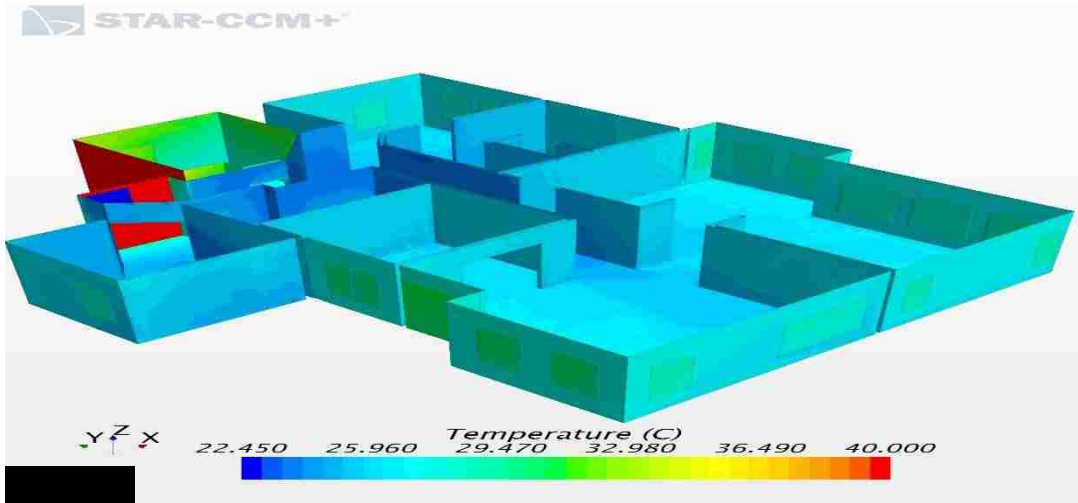
5.6.1 Temperature Distribution

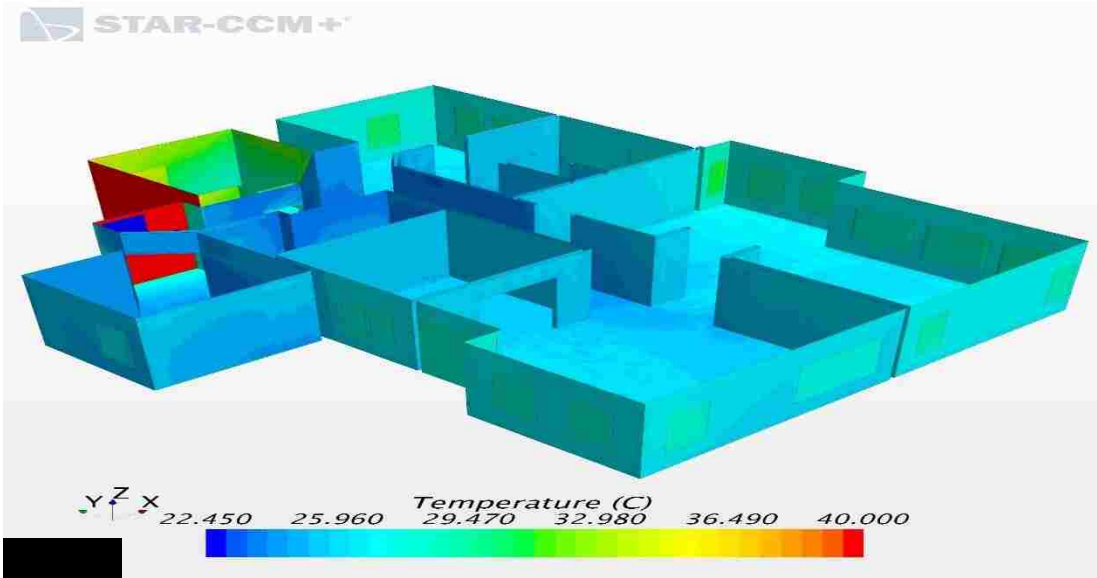
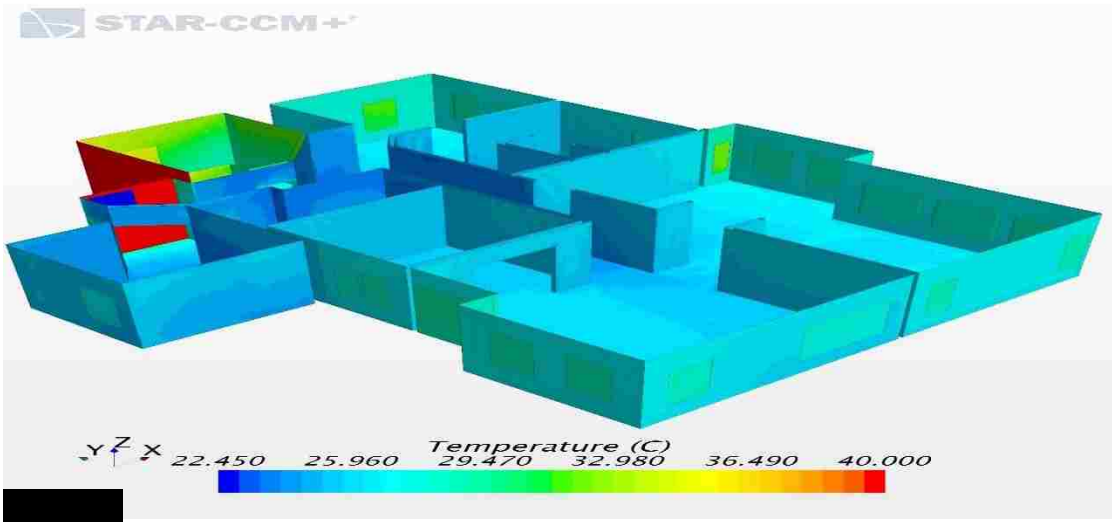
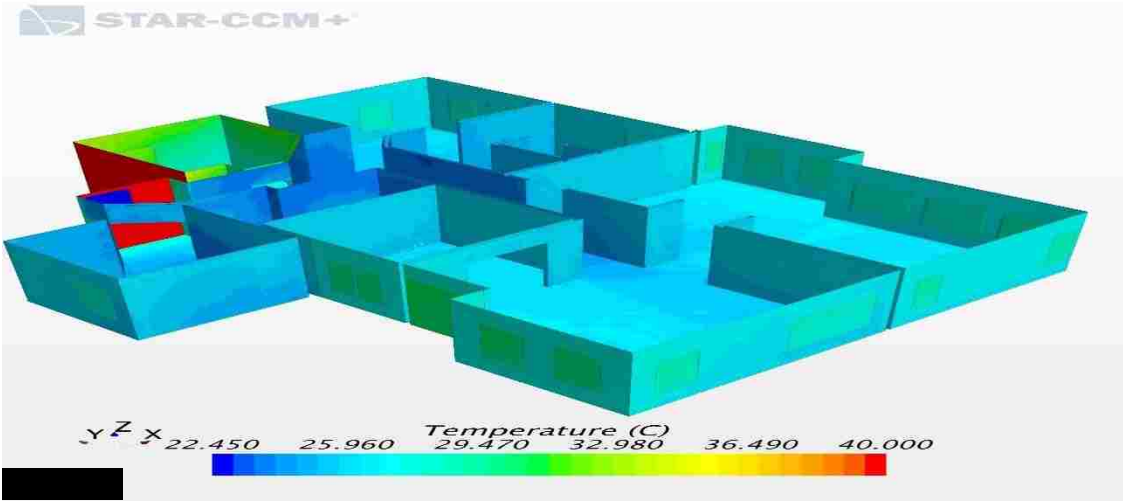
As it is represented in Figure 5.7, 5.8, 5.9 and 5.10, the temperature distribution in windows, external and internal walls and doors are evaluated in three different hours (12, 3 and 5 p.m.). As it can be observed in the figures, the temperature range is similar in different hours of a day. However, there are differences in the amount of radiation observed by windows and doors since the solar radiation is variable during a day because the position of the sun is changing in different hours. In this regard, at midday, the sun is positioned high in the sky and the paths of the sun's rays through the earth's atmosphere is shortened and consequently, less solar radiation will be absorbed or scattered by the earth's atmosphere and more radiation reaches the earth's surface. This theory is verified with the result of CFD simulation and as it is represented in Table 6.4 the total solar radiation that reaches the external walls, windows and doors is higher at 12 p.m. This means that there is a more critical situation in the midday and the criteria of design should be obtained in respect to the condition of the building in the most critical situation.

Table 5. 4. Values of the incident solar radiation on the building.

| Time | Radiation Heat Flux (W/m ²) |
|---------|---|
| 12 p.m. | 1291.9 |
| 3 p.m. | 1286.2 |
| 5 p.m. | 1209.37 |

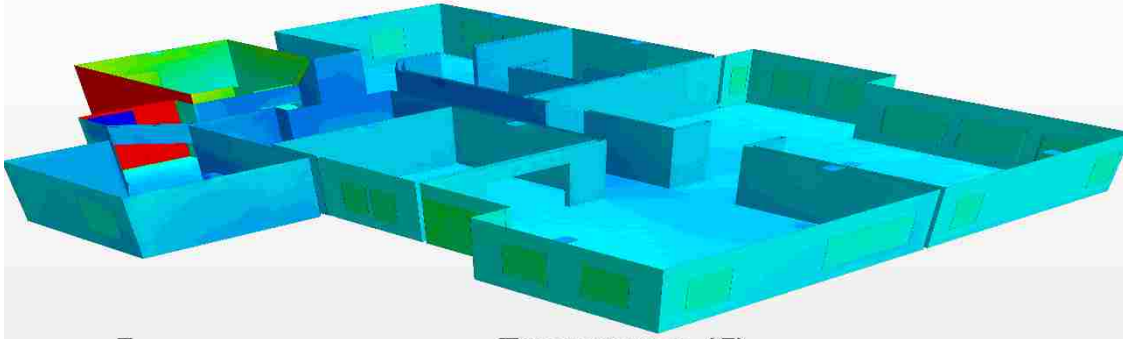








STAR-CCM+

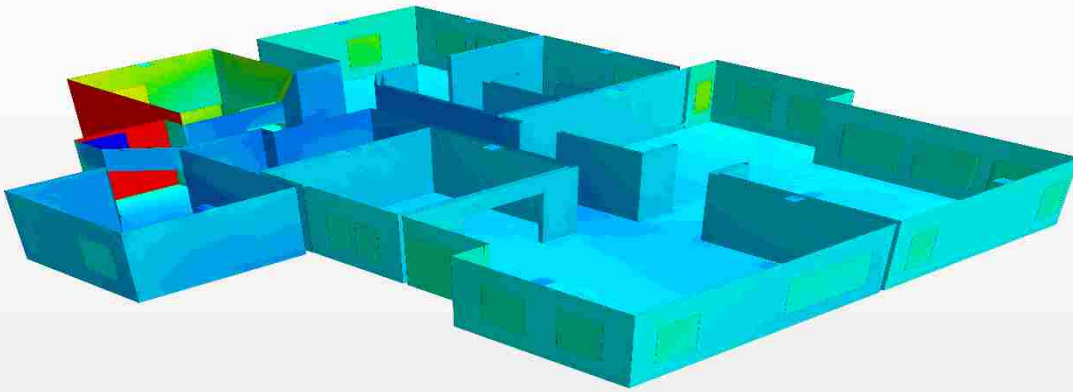


y z x

22.450 25.960 29.470 32.980 36.490 40.000



STAR-CCM+

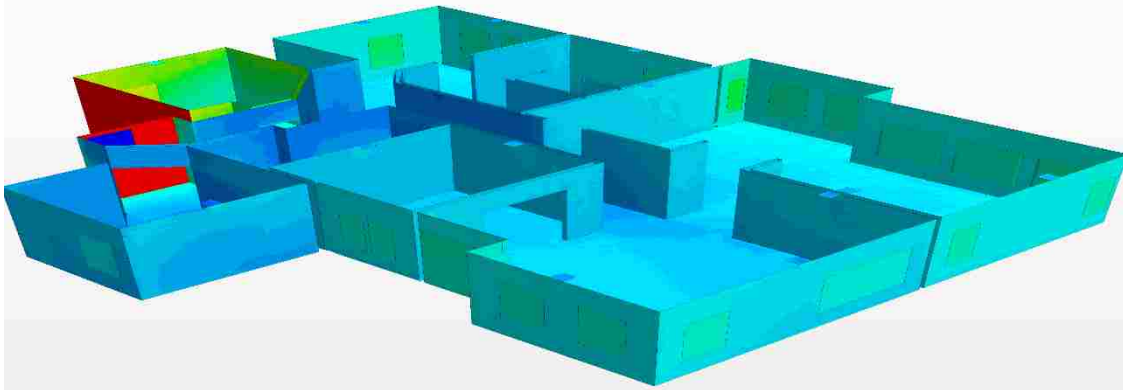


y z x

22.450 25.960 29.470 32.980 36.490 40.000



STAR-CCM+

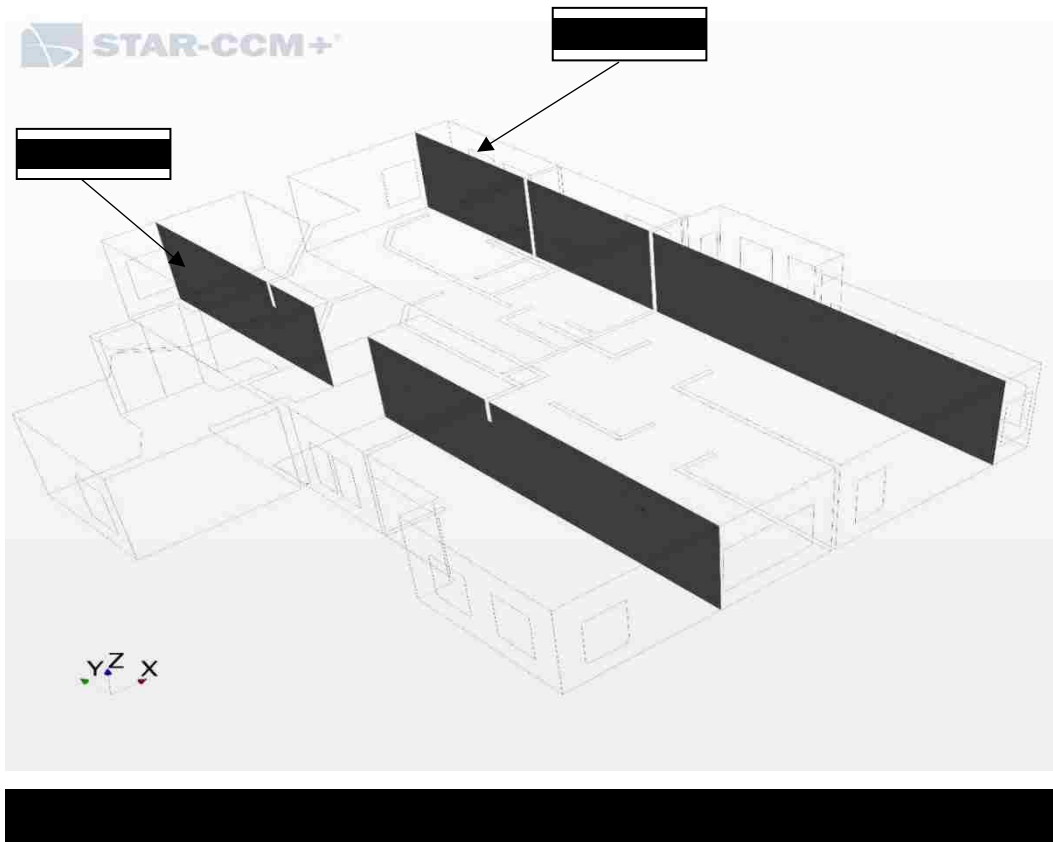


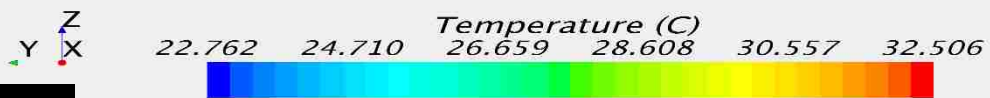
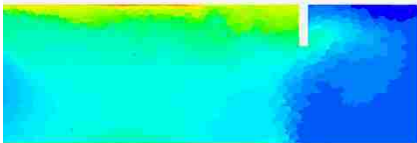
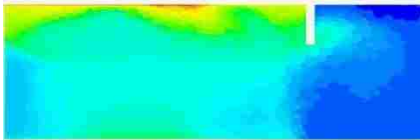
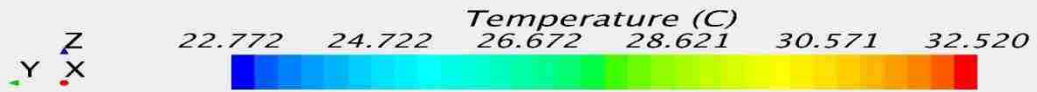
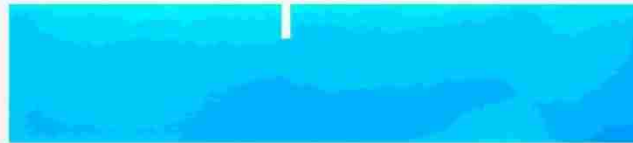
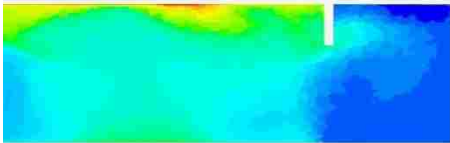
y z x

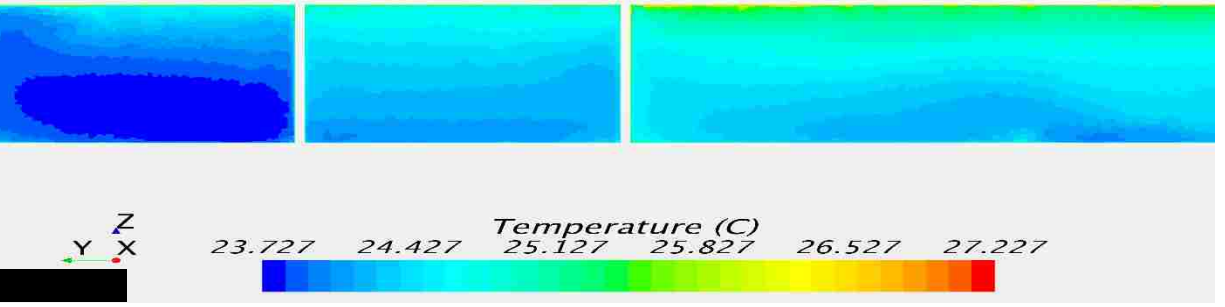
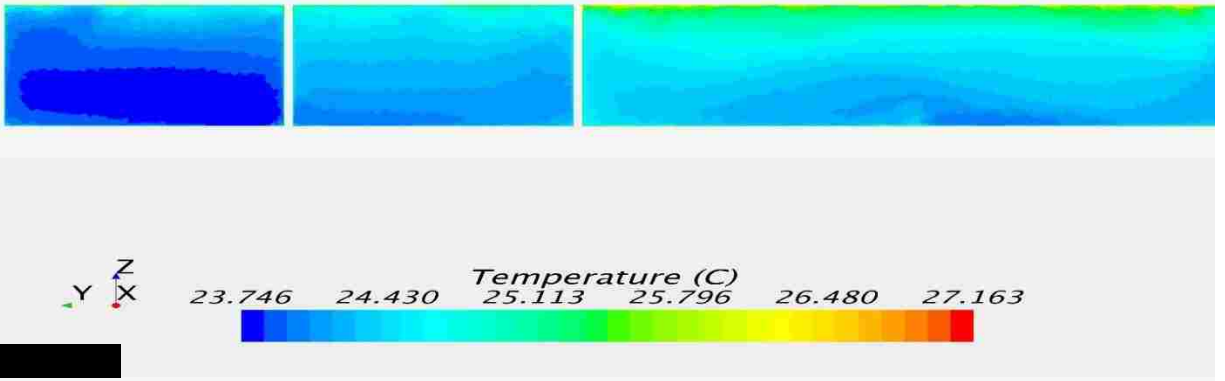
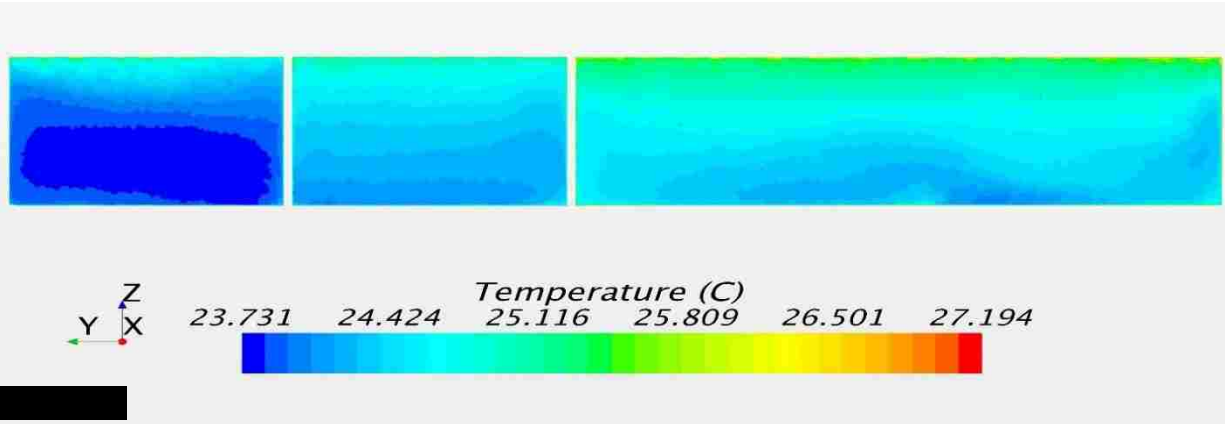
22.450 25.960 29.470 32.980 36.490 40.000

5.6.2 Temperature Profiles in Two Main Sections

As it has been shown above, the condition is the same in all 4 strategies and the most critical condition is at 12 p.m. In this regard, the temperature profiles are evaluated only at 12 p.m. and as represented in Figure 5.11, the temperature profile for each strategy is evaluated in two main sections of the house. The results can be observed in Figure 5.12, 5.13.







The temperature maintained in the four strategies seems to be in the comfort zone. However, to conclude the best strategy for better thermal comfort, it is necessary to consider humidity and velocity distribution as well, which will be described in the following sections.

5.7 Humidity Track

One of the main goals of the current study is tracking humidity node by node through a complex model. It is important to know that the percentage of relative humidity is consequently changed as the ventilated cold air goes through each section. Typically, the relative humidity control in the building, where evaporative systems are used is mandatory. The humidity will be tracked with a field function using the below formulas for an ideal gas.

Relative humidity is the ratio of the partial pressure of water vapor to the equilibrium vapor pressure of water at the same temperature. Therefore, the relative humidity is a function of pressure and temperature.

$$RH (P, T) = \frac{\text{Partial Pressure}}{\text{Equilibrium Pressure}} \quad (5.1)$$

The equilibrium pressure is a pressure that a vapor exerts in thermodynamic equilibrium with its condensed phases at a given temperature. In another word, at the equilibrium pressure RH=100% at a given temperature. One of the most well-known equations for obtaining equilibrium pressure is Antoine Equation, which is represented as follows:

$$\log_{10}^p = A - \frac{B}{C+T} \quad (5.2)$$

Where

p = Equilibrium Pressure

T =Temperature in Celsius

A, B, C = Component specific constants

The above-mentioned equation is only appropriate for pure components. The constants for pure water are represented in Table 5.5.

Table 5.5 Antoine Equation Constants.

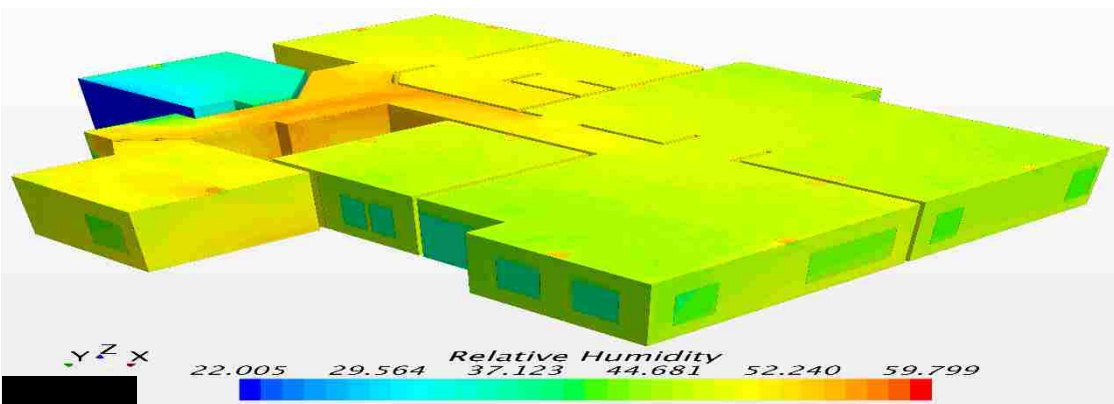
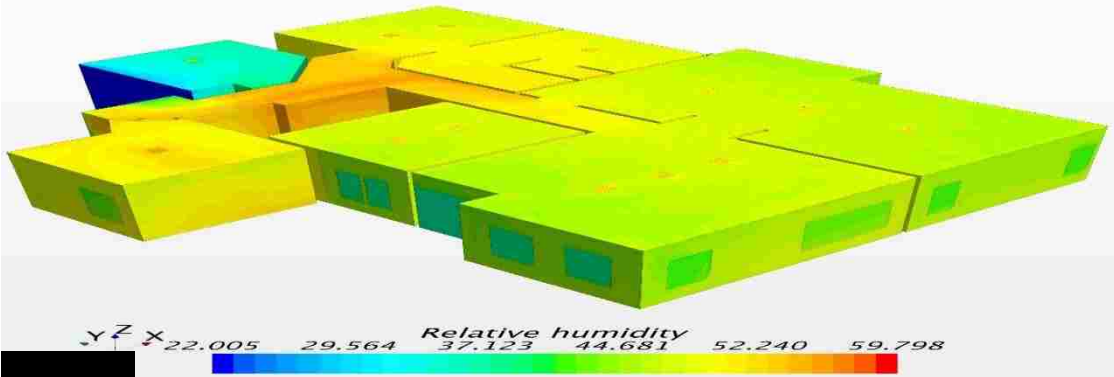
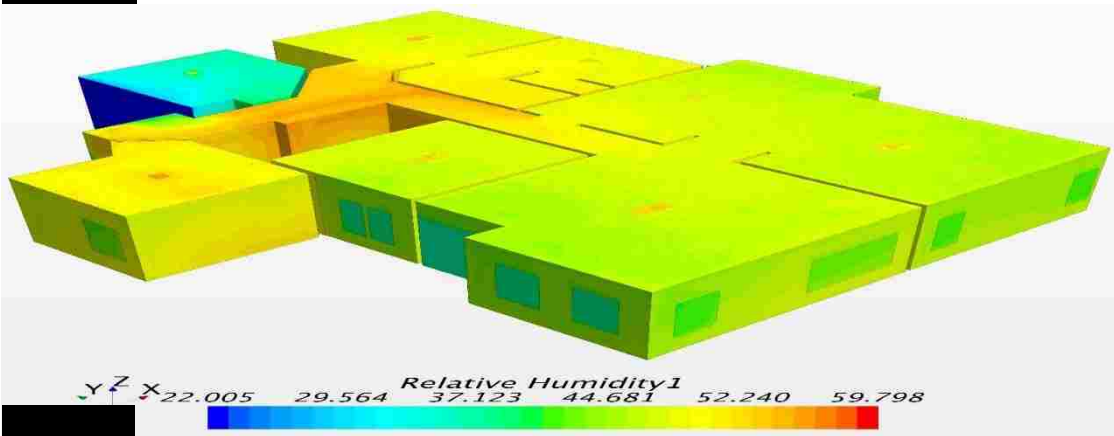
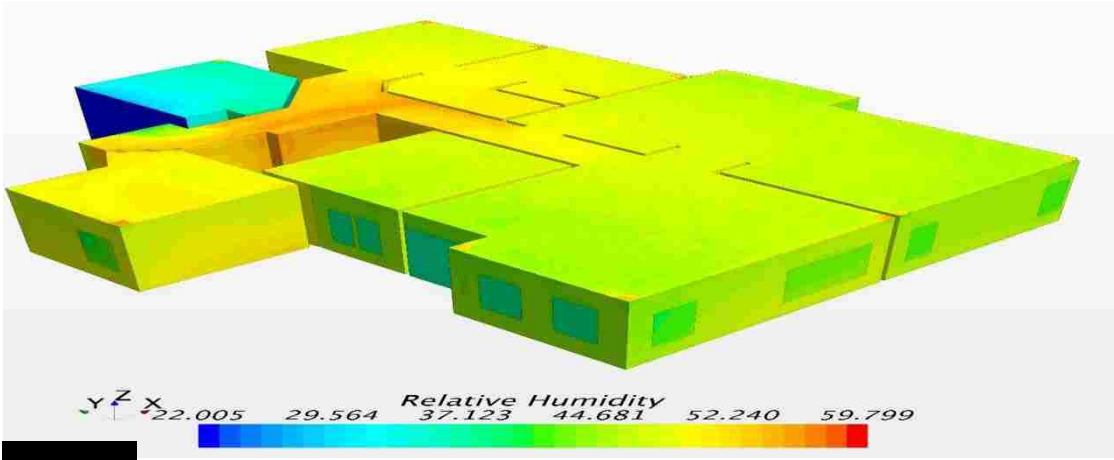
| | A | B | C | Tmin (C) | Tmax (C) |
|-------|---------|---------|---------|----------|----------|
| Water | 8.07131 | 1730.63 | 233.426 | 1 | 100 |
| Water | 8.14019 | 1810.94 | 244.485 | 99 | 374 |

Moreover, the partial pressure of water vapor can be calculated as:

$$Partial\ Pressure = \frac{Component's\ Pressure}{Absolute\ Pressure} \quad (5.3)$$

However, using Dalton's law for an ideal gas, we can conclude that if the pressure is constant then the fraction of partial pressure is the same as mole fraction. Therefore, changes in the mass fraction of water vapor in the mixture can be calculated.

Humidity profile through the entire house and two main sections for four various strategies are represented in Figure 5.14, Figure 5.15 and 16.

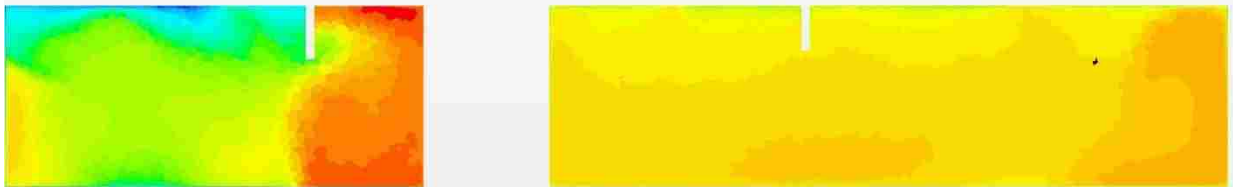




Z
 $Y \ X$ *Relative Humidity*
 33.038 38.166 43.294 48.422 53.550 58.678



Z
 $Y \ X$ *Relative Humidity*
 33.154 38.250 43.346 48.441 53.537 58.632

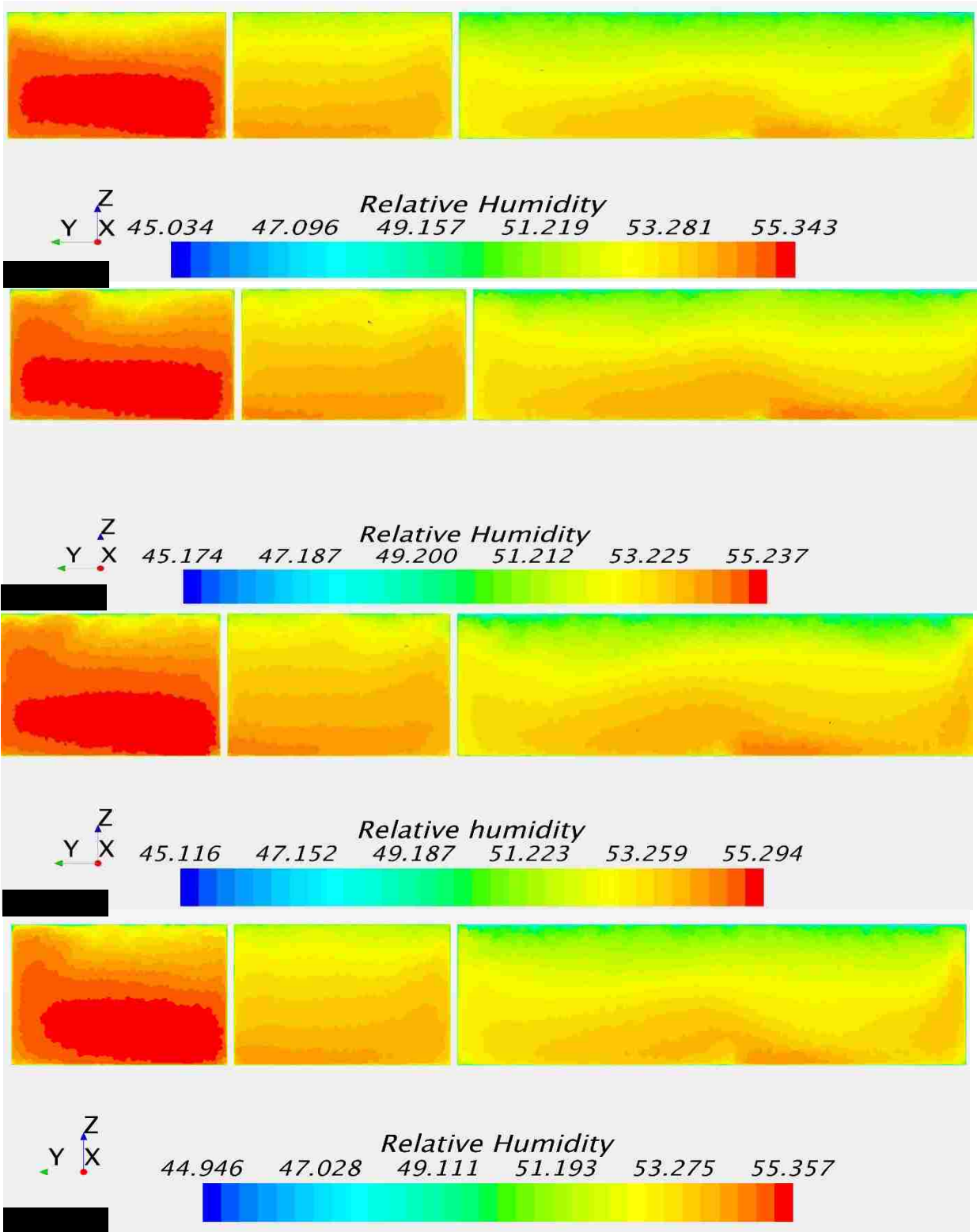


Z
 $Y \ X$ *Relative humidity*
 33.200 38.297 43.394 48.491 53.588 58.685



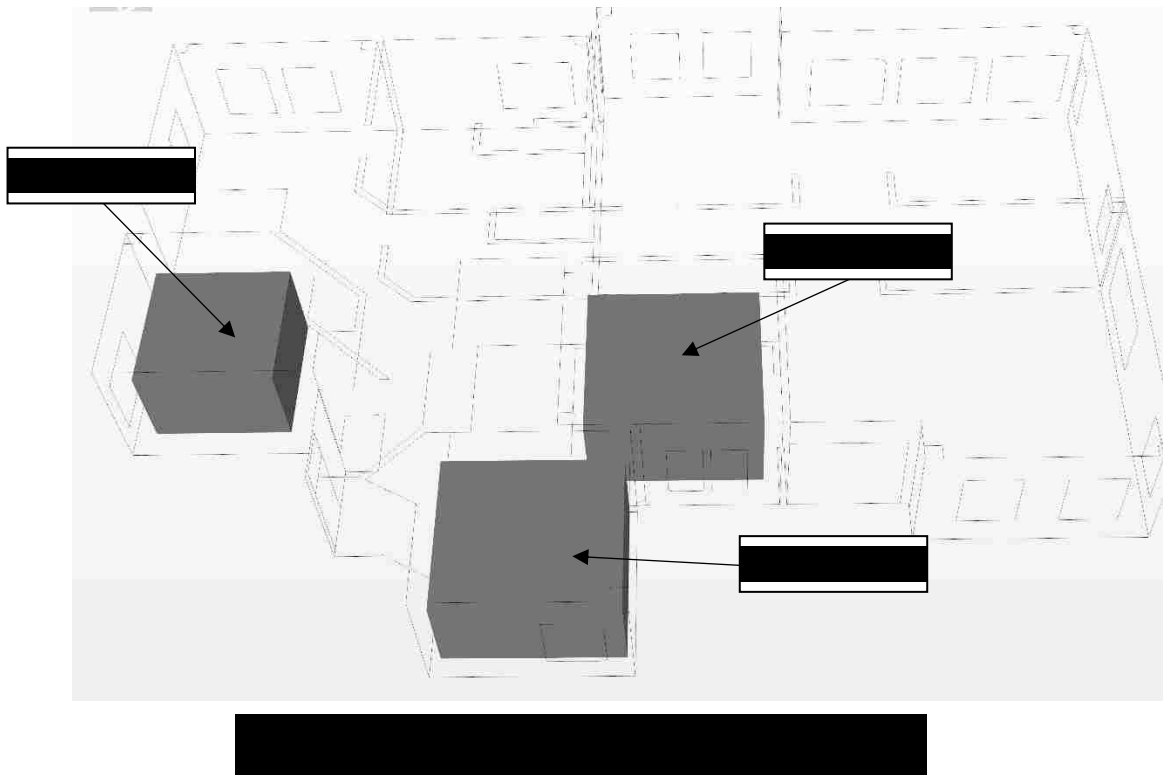
Z
 $Y \ X$ *Relative Humidity*
 33.181 38.279 43.377 48.475 53.573 58.671





As it has been shown in the Temperature and Humidity profiles section, the humidity and temperature distributions are really close for different strategies in different sections, which means the heating and cooling loads are calculated appropriately. However, to be able to use a system in a building, it should be evaluated regarding thermal comfort based on the ASHRAE thermal comfort standard and the differences will be shown in the following section. In this regard, the most critical conditions are evaluated. As the rooms locations are shown in Figure 5.17, the Bedrooms 1, 2 and 3 have most critical situations, which are described as follows:

1. Bedroom 1 is one of the two closest rooms to the inlet of the evaporative cooler. Since the entrance of this bedroom is in contrast with the direction of the inlet and because of the small distance from the inlet and having an adjoined wall to the garage, which is an unventilated space, the evaluation of the condition of this room is one of the necessities.
2. Bedroom 2 is another room with a small distance from the outlet and the entrance of the room is just in front of the inlet. The temperature and relative humidity should be evaluated in this room exclusively. In other words, providing thermal comfort in this room is a concern.
3. Bedroom 3 is the other critical section since it is far from the inlet and the direction of the entrance of the room is in the opposite direction. It affects the ventilated air flow direction completely and providing thermal comfort is more difficult.



5.8 Thermal Comfort

As it has been elaborated in section 1.3, to provide thermal comfort in a building, the total condition of spaces should be evaluated in respect to Thermal sensation, Comfort Zone, and Draft Rate. As it is mentioned in the previous section, thermal comfort should be addressed in the most critical spaces (Bedroom 1, 2 and 3). In this regard, these terms are evaluated for these three spaces to conclude the best strategy for the outlets.

As it is represented in Figure 5.17, three blocks with a height of 2 m are considered for these critical spaces. The reason for setting 2 m height is that since we need to evaluate thermal comfort in the building, providing condition up to the height of 2 m would be logical since the residents of the building are living at this level and the average height of people would be considered 1.75 m based on ASHRAE thermal comfort standard.

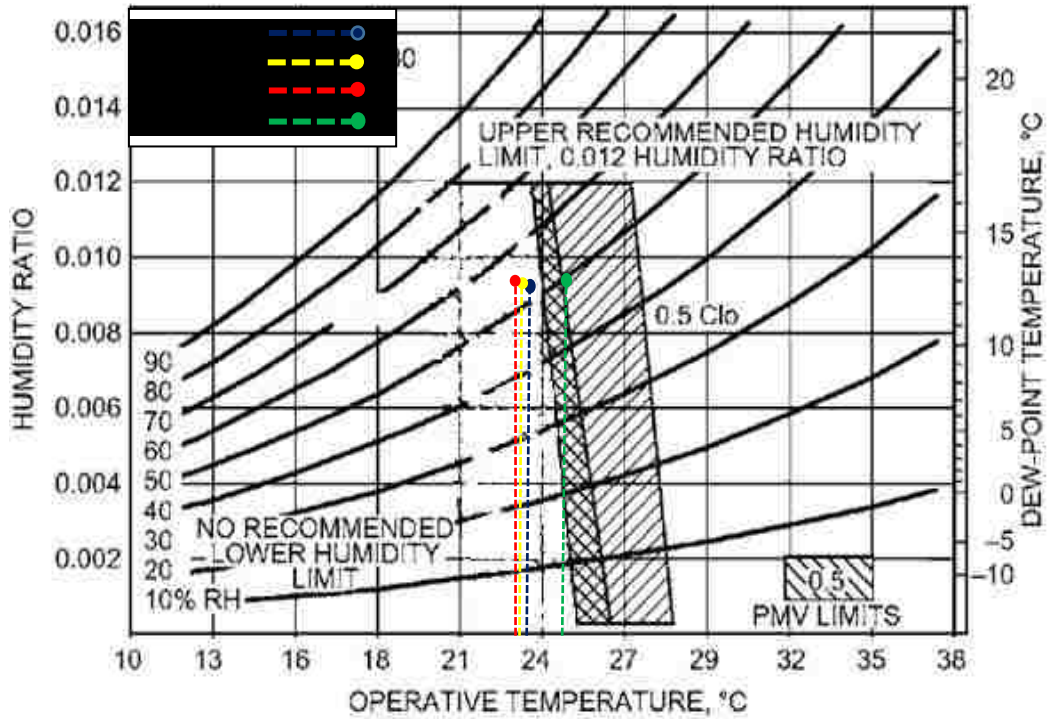
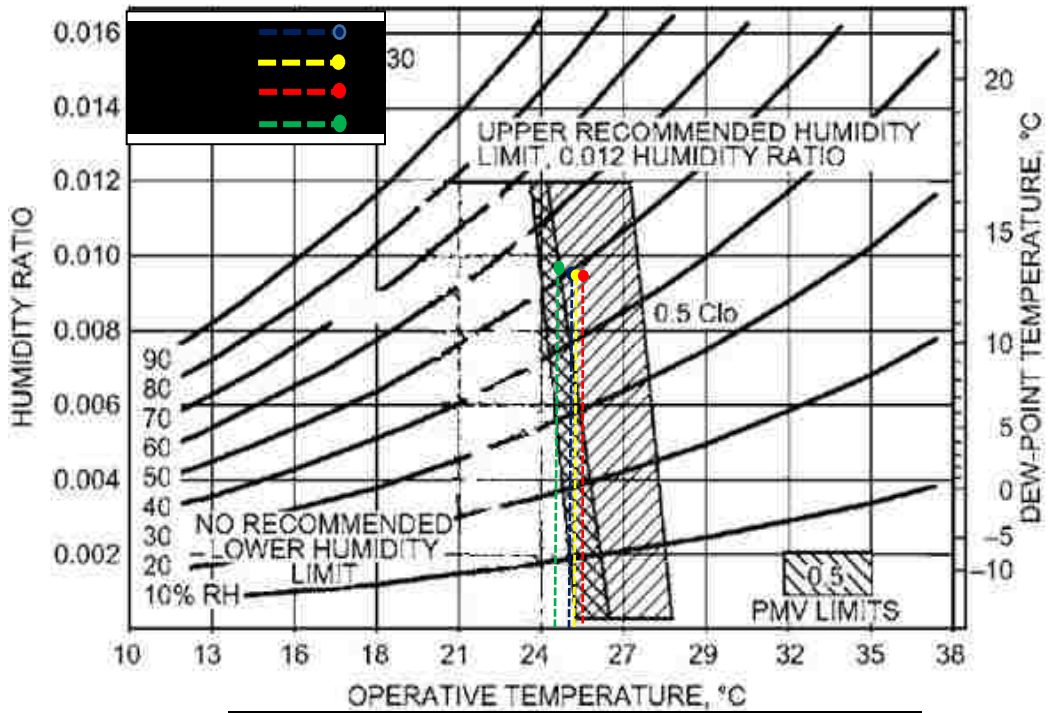
5.8.1 Summer Comfort Zone Evaluation

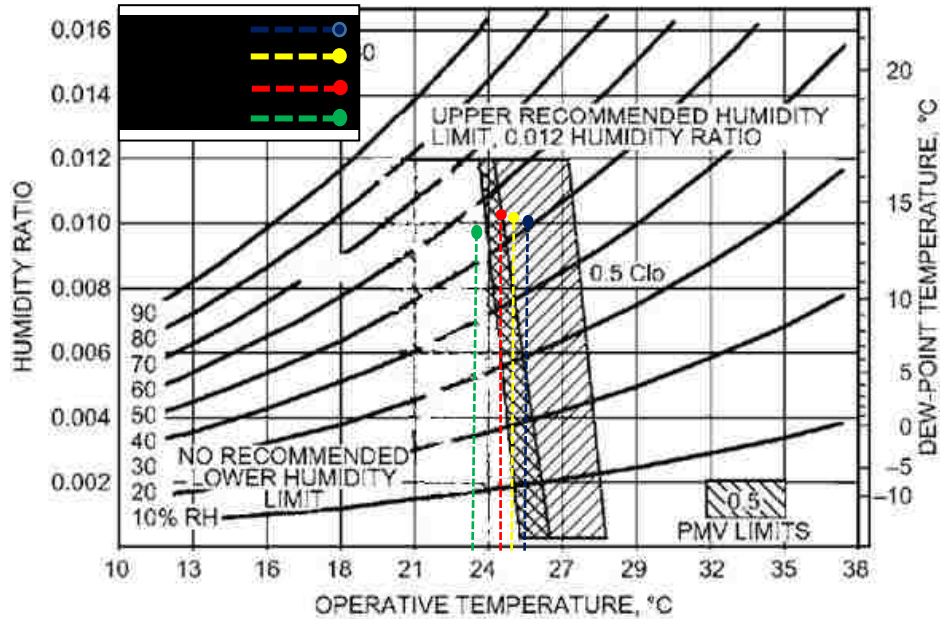
The three above mentioned critical situations have been evaluated based on the Comfort Zone standard presented by ASHRAE standard 55. In this regard, the average temperature and humidity in the three mentioned blocks in the Figure 5.17 will be verified for the four strategies with comfort zone standard as the first step to distinguish the best strategy of outlets in the building. The mean conditions are represented in Table 5.6 and compared with each other in Figure 5.18, 5.19 and 5.20.

Table 5. 6. Average Temperature And Humidity For Blocks With 2 m Height.

| Strategy | Bedroom 1 | | Bedroom 2 | | Bedroom 3 | |
|----------|----------------|-----------------------|----------------|-----------------------|----------------|-----------------------|
| | Temperature °C | Relative Humidity (%) | Temperature °C | Relative Humidity (%) | Temperature °C | Relative Humidity (%) |
| A | 25.62 | 49.5 | 23.71 | 55.38 | 24.55 | 52.66 |
| B | 25.66 | 49.37 | 23.68 | 55.51 | 24.47 | 52.93 |
| C | 25.68 | 49.33 | 23.67 | 55.52 | 24.4 | 53.14 |
| D | 24.52 | 52.77 | 25.5 | 49.7 | 23.68 | 55.5 |

As represented in Figure 5.18, 5.19 and 5.20 in Bedroom 1, the air condition is obtained in Summer Comfort Zone in all strategies, which means all strategies will follow the standard in providing summer comfort in Bedroom 1. For Bedroom 2, only **strategy D** obeys Summer Thermal Comfort standard and strategy A, B and C are out of the Summer Thermal Comfort Zone and it can be concluded that **strategy D is the best strategy in this section**. However, in Bedroom 3 all strategies are in the Summer Comfort Zone except the strategy D. As a conclusion, **strategy D** is the best for Bedroom 1 and 2, however for Bedroom 3, strategy A is the best since it is in the middle of the zone. In this regard, other factors should be evaluated to find the best strategy.



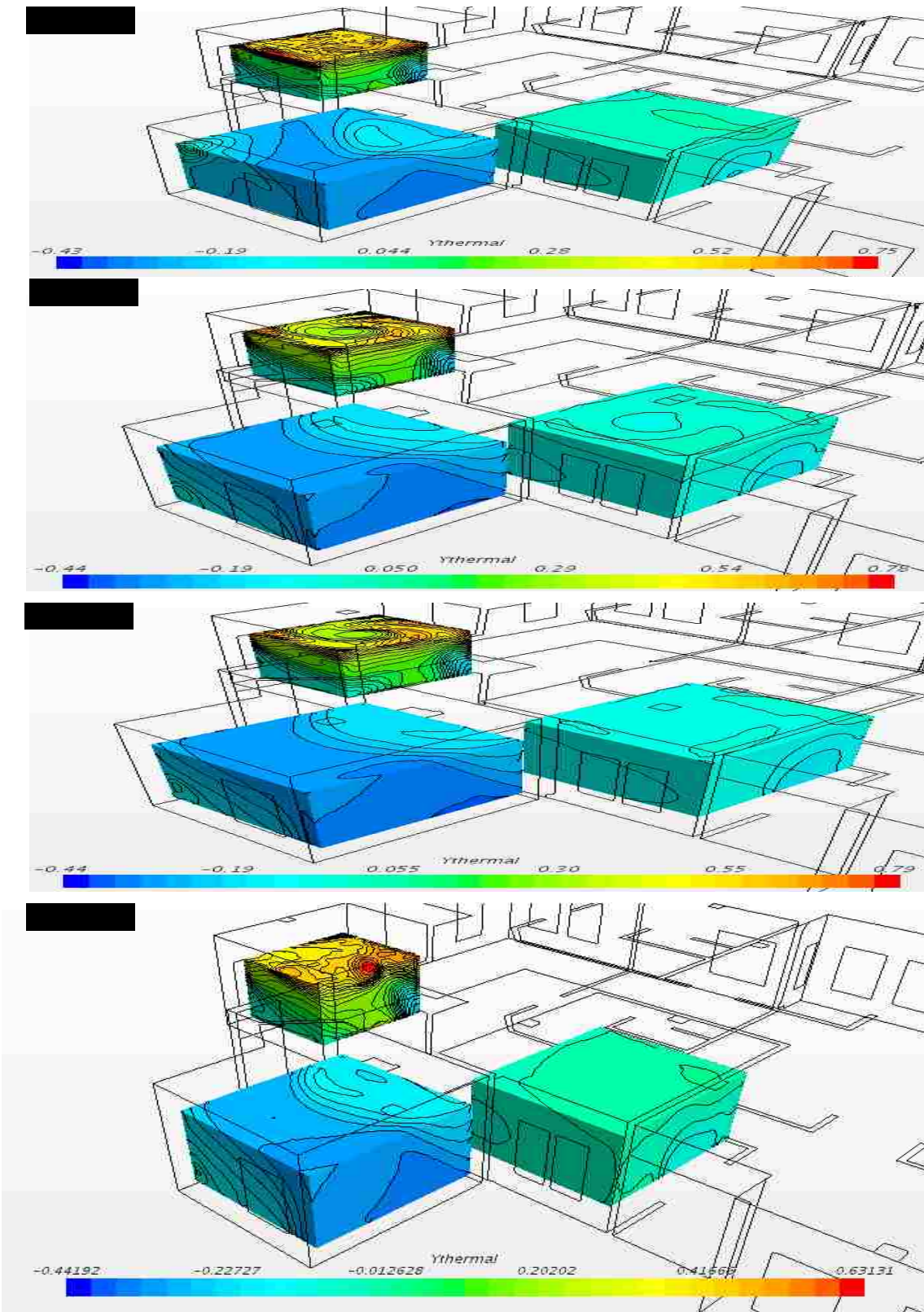


5.8.2 Thermal Sensation

As it has been shown in comfort zone results in section 5.8.1, the **strategy D** meets the standard of thermal comfort better (in Bedroom 1 and 2 and close enough in Bedroom 3) for obtaining the air condition in the summer comfort zone in critical spaces; however, these strategies should be evaluated in respect to Thermal Sensation and Draft Rate as well. The results of thermal sensation are tabulated in Table 5.7 and shown in Figure 5.21.

Table 5. 7. Mean Thermal Sensation In Critical Spaces.

| Strategy | Bedroom 1 | Bedroom 2 | Bedroom 3 |
|----------|-----------|-----------|-----------|
| A | 0.1 | -0.16 | -0.05 |
| B | 0.21 | -0.27 | -0.07 |
| C | 0.218 | -0.272 | -0.1 |
| D | -0.06 | 0.17 | -0.27 |



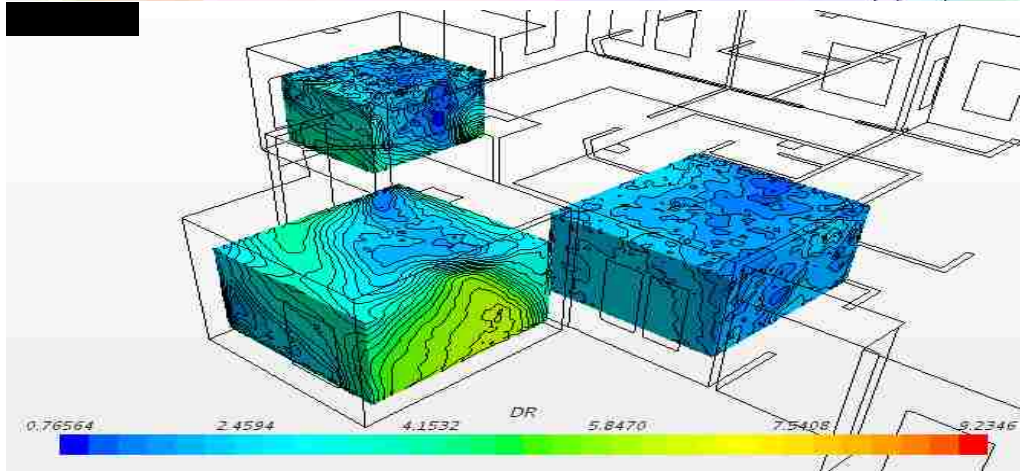
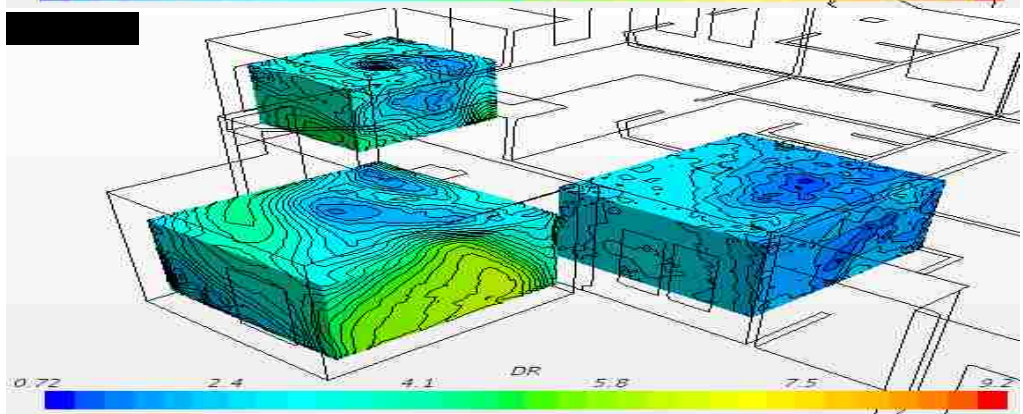
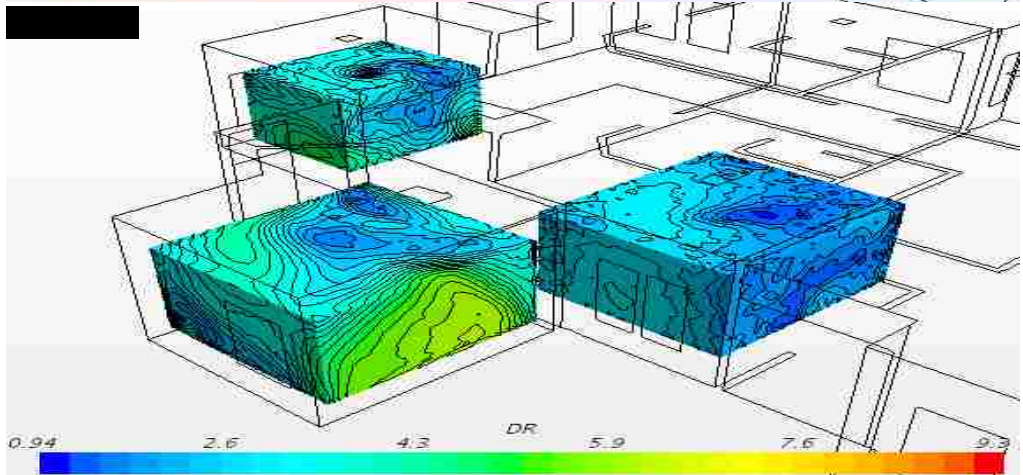
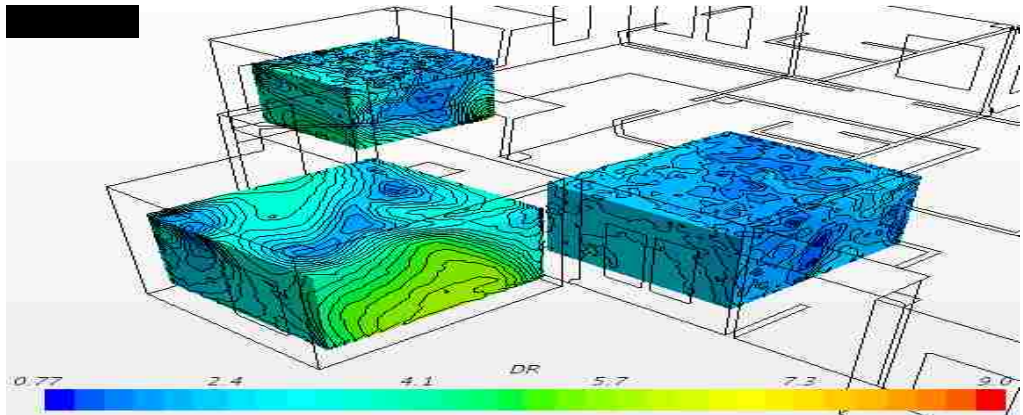
As it can be concluded from the above table and figure, from the Thermal Sensation point of view, strategy A is more appropriate in Bedroom 2 and 3 in comparison with the other strategies since the results show that in strategy A, the thermal sensation is closer to neutral condition (Thermal Sensation=0), which is the ideal case. However in Bedroom 1, strategy D is more appropriate one. To summarize, **Strategy A** is more appropriate in Thermal Sensation aspect.

5.8.3 Draft Rate Evaluation

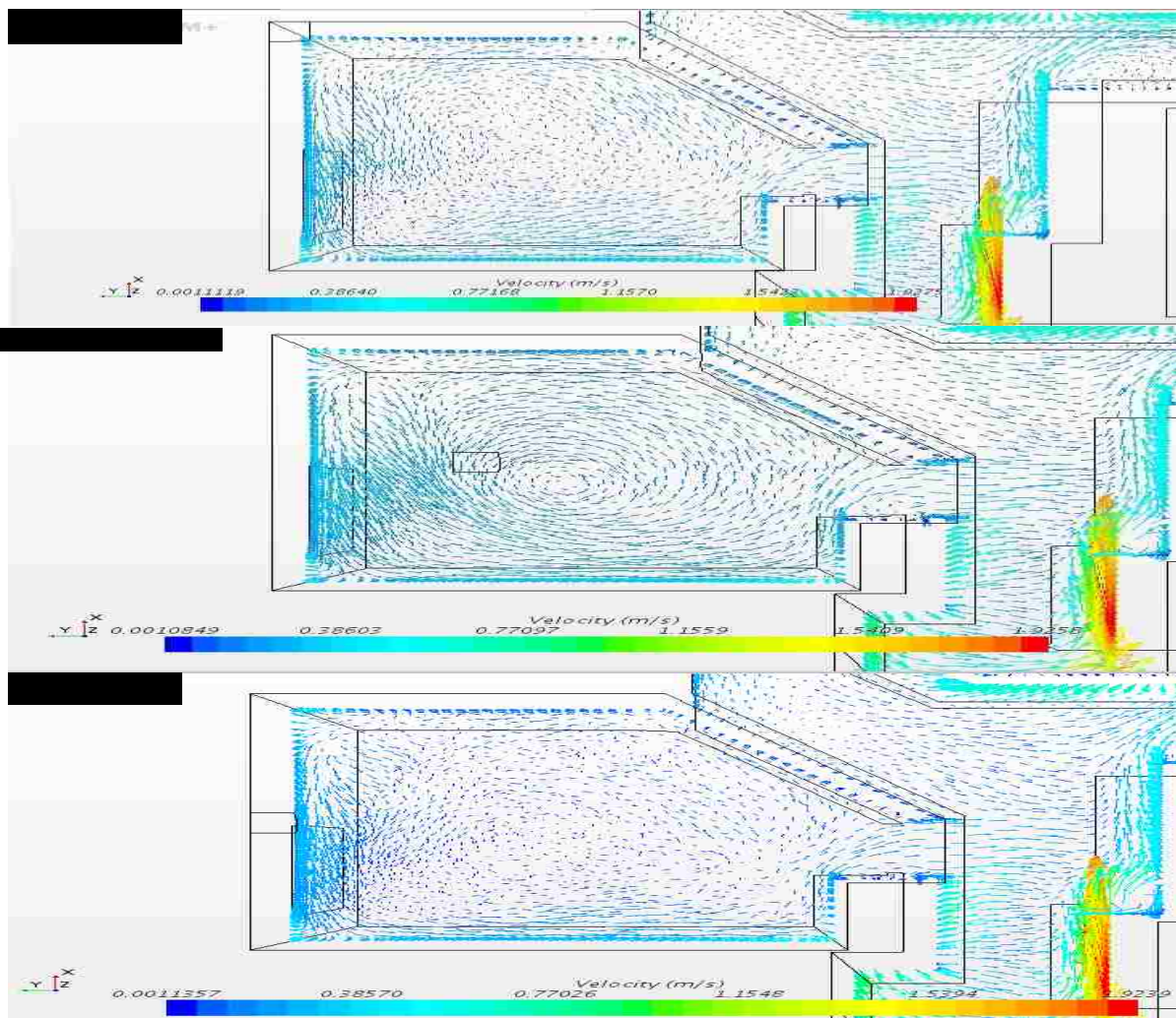
Calculating the Draft Rate is the last step in evaluating thermal comfort in the building. As it has been mentioned in section 1.3.3, the air velocity has a key role in providing thermal comfort and can easily deteriorate the Thermal Sensation and Comfort Zone results since it can cause undesired air movement in the building. The DR creates discomfort although the temperature and the amount of humidity are appropriate in the building. The results of DR are tabulated in Table 5.8 and represented in Figure 5.22.

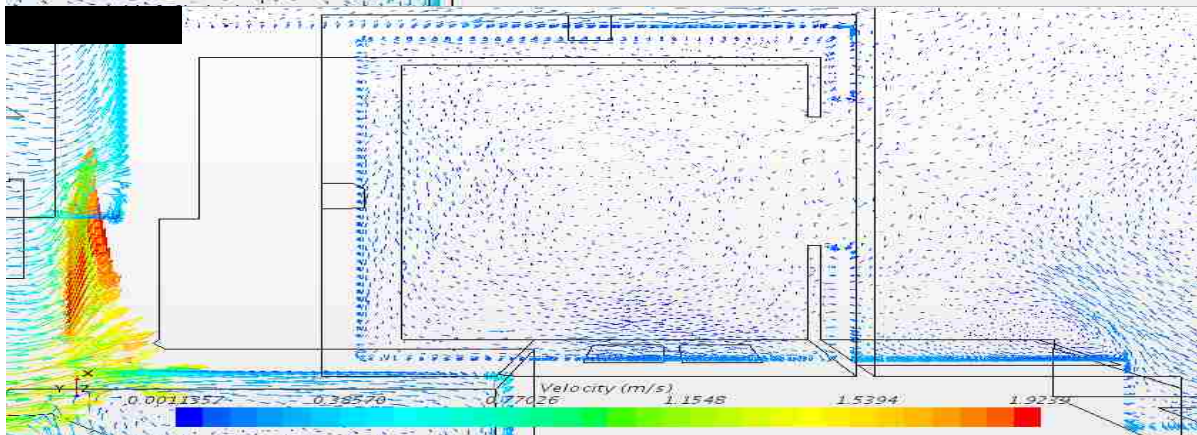
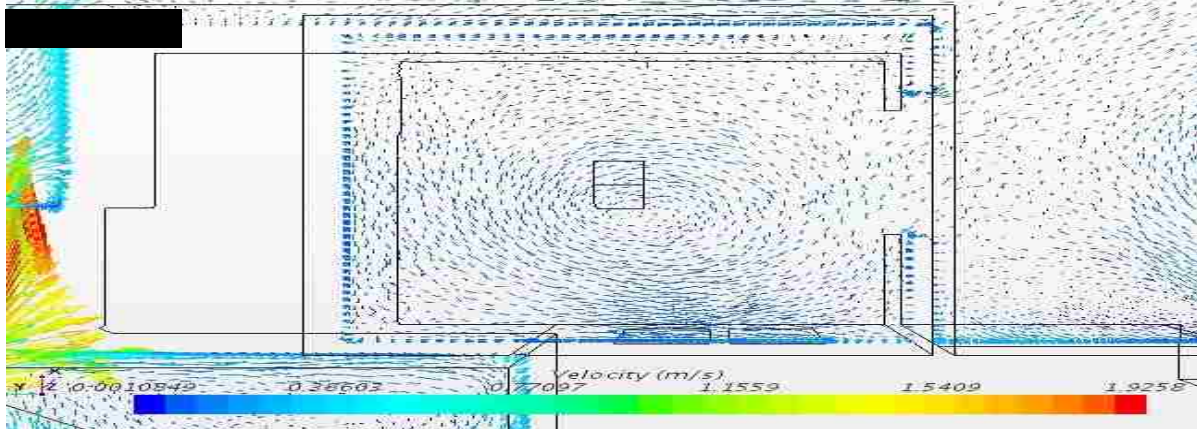
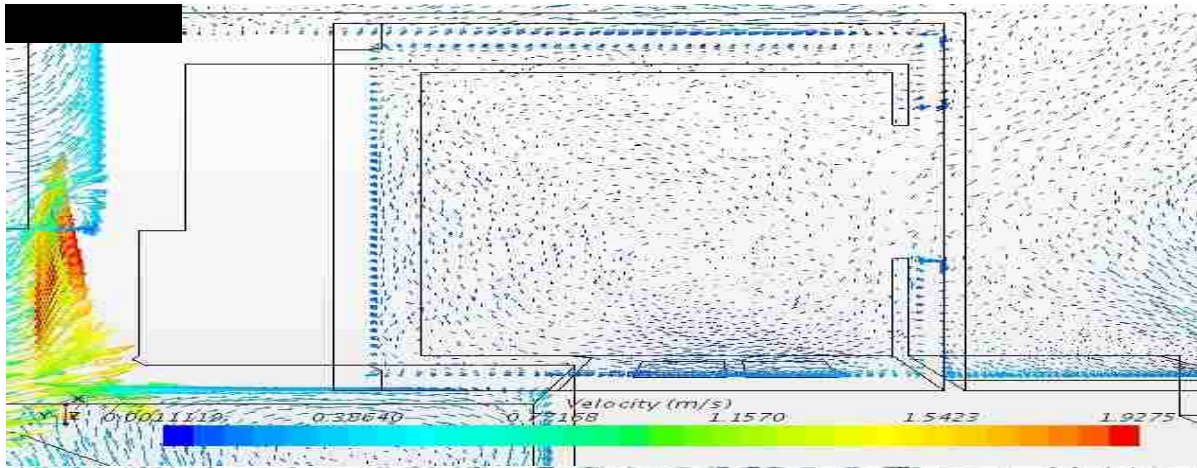
Table 5. 8. Mean Draft Rate In Critical Spaces.

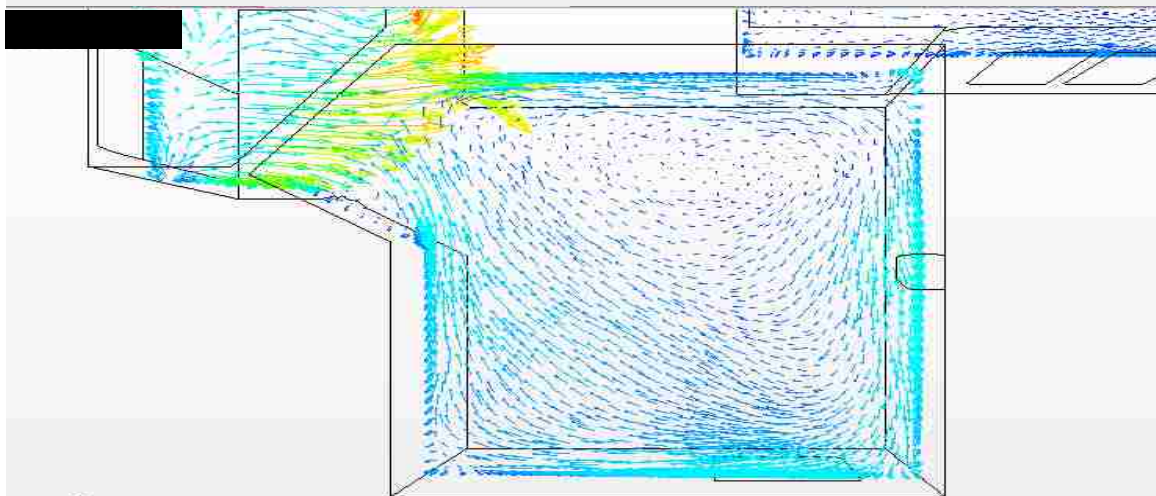
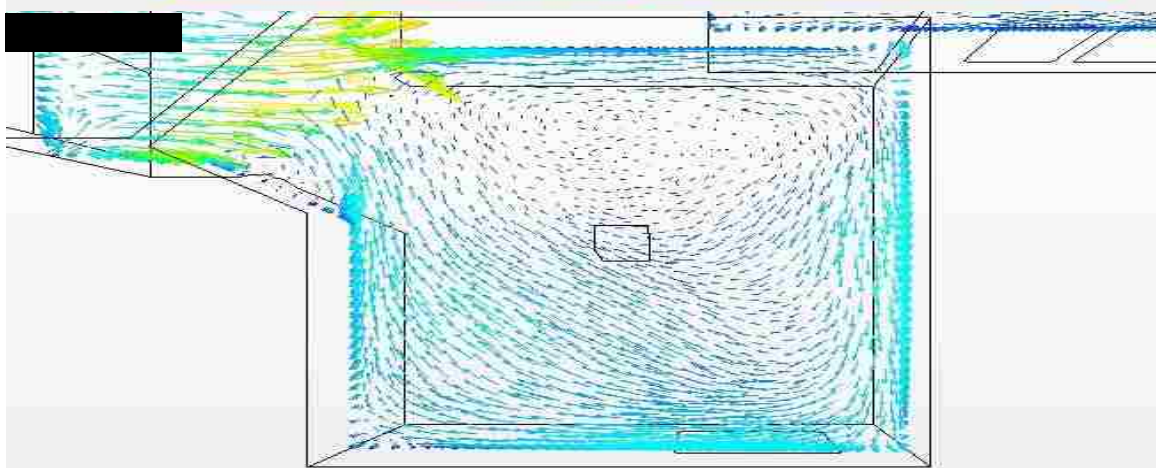
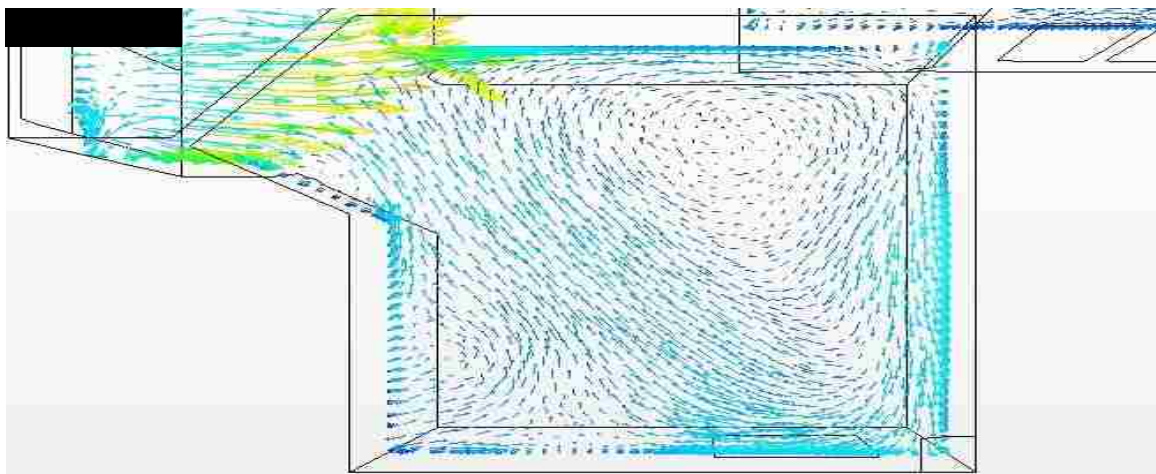
| Strategy | Bedroom 1 | Bedroom 2 | Bedroom 3 |
|----------|-----------|-----------|-----------|
| A | 2.9 | 3.7 | 1.9 |
| B | 3.3 | 4.1 | 2.2 |
| C | 3.2 | 4.08 | 2 |
| D | 1.94 | 2.7 | 4 |



As it can be observed in Table 5.7 and Figure 5.22, there is lower Drat Rate in strategy D in Bedroom 1 and 2 in respect to other strategies, however in Bedroom 3, strategy A is the best. As a conclusion in DR point of view, **strategy D** is more appropriate in respect to other strategies and the percentage of dissatisfaction is less than the others. Although all strategies are below the DR limit, providing less DR provides a more appropriate condition in the building. In addition, the flow direction is represented in Figure 5.23, 5.24, and 5.25 asserting that there is lower air movement in the center of Bedroom 1 using strategy A or D, and because of the outlets locations, lower swirl flow is created in the living spaces. Therefore, the DR definition can be validated by the behavior of flow in the building as well.







CHAPTER 6

CONCLUSION AND SUGGESTIONS

6.1 Conclusion

This research study was carried out to investigate the influence of exhaust air vents (Outlets) on the thermal comfort, indoor air satisfaction, and clarifying how the simplest details, like the location of air conditioning systems can provide more comfort in residential and industrial buildings. With the employment of the Realizable $k-\varepsilon$ model and using STAR-CCM+, the thermal comfort environment of a CAD model with an evaporative cooling system is investigated and compared respect to various strategies for outlets. With the strong CAD Software, SolidWorks, a complex model was generated and numerical study on the different sections of the model were shown with STAR-CCM+ and validated with a paper published in the energy conservation field. It can be concluded that proper inlet condition, and fine mesh generation at inlet and outlets are essential for accurate CFD simulation, using the Realizable $k-\varepsilon$ model. The results showed the reliable ability of STAR-CCM+ to calculate flow features and powerful compatibility to add the desired definition, such as relative humidity tracking as an external field function in STAR- CCM+.

In the numerical study of the effects of outlets for the CAD model, we can conclude from the temperature and relative humidity profiles that the air inside the test space is distributed very well in different sections, which confirms the good selection of the inlet location and the number of outlets assumed for each room.

In the first step, the results were evaluated for the entire model for each of the strategies concluding that the mean conditions for all of the strategies are acceptable based on ASHRAE

Thermal Comfort standard. However, more precise investigations were needed in the critical sections of the house.

In the next step, temperature and relative humidity profiles were evaluated in the two main sections of the building. These sections are in the middle of front and back rooms in respect to the location of the inlet. It can be observed that we are faced with the critical condition in the frontal section in temperature, relative humidity percentage, and air distribution. In this regard, the most critical locations have been defined that are the rooms close to the inlet, a room, which is far from the inlet and the entrance of the air into the space is in opposite direction in respect to the outlet.

After determining the most critical spaces in providing thermal comfort, those spaces were evaluated in respect to various criteria needed to provide thermal comfort, and they were compared based on Comfort Zone, Thermal Sensation, and Draft Rate.

In Comfort zone evaluation, **strategy D** showed to be a more appropriate condition for critical spaces (appropriate for 2 out of 3 critical spaces) since it is much closer to the desired condition for thermal comfort based on the Comfort Zone graph. However in Thermal Sensation evaluation, **strategy A** is closer to ideal condition in respect to other strategies. Strategy A results showed that the thermal sensation is closer to 0 value, which means the neutral condition is dominant and more appropriate in the spaces. As the last step, the strategies were evaluated based on Draft Rate, which is much more important than Comfort Zone and Thermal Sensation aspects, since the swirl flow, and inappropriate air distribution in the spaces causes an unacceptable sense of cooling on some parts of body such as the neck, head, ankle and leg region. In other words, sensitivity to draft is greatest where the skin is not covered by clothing. As it was observed in the results, swirl flow is dominant much more in strategy B and C rather

than A and D, which asserts that the strategy A or D should be selected to prevent unwanted local cooling more. However, **strategy D** is the best, which meets the Thermal Comfort criteria more appropriately.

Based on the all results, we can conclude that in the air conditioning of buildings not only selecting appropriate systems based on cooling load of the building is necessary, but also investigation regarding inlet and outlet vents locations is a must, and we can conclude that the **location on the ceiling and on the intersection of the farthest wall from the entrance of each space would be the best location we can consider for exhaust air vents (Strategy D).**

6.2 Further Work

1. In the current study, the attic has been assumed to be an unventilated space. However, since the exhaust air will be entered into the attic, the air temperature in the attic will be less than the unventilated assumption. Therefore, the attic can be added to the flow geometry to track its effects on energy conservation inside the building.
2. Modeling of contaminant species is needed to be evaluated. In the current study, no air contaminants are assumed at the inlet and the effect of these particles in the flow direction and temperature distribution is needed to be evaluated in further research.

3. In the current study, all spaces are assumed to be empty with no residents and no real-life simulation. Much like in reality, electronic tools such as desktops, TVs and home furnishings, such as tables and chairs and human beings should be included in the simulation.

4. The same problem needs to be solved for thermal comfort in the winter time. The results must be evaluated for different strategies and compared with the results shown in the current study.

REFERENCES

- [1] ASHRAE Standard 55-2013: Thermal Environmental Conditions for Human Occupancy
- [2] ASHRAE Standard 62.1-2013: Ventilation for Acceptable Indoor Air Quality
- [3] ASHRAE Handbook Fundamentals, 2013. American Society of Heating, Refrigerating and Air Conditioning Engineers, SI Edition, Chapter 5.
- [4] Evaporative Air-conditioning: Applications for Environmentally Friendly Cooling, Volumes 23-421
- [5] B. Chenari, J. Carrilho, M. Silva, Towards sustainable, energy-efficient and healthy ventilation strategies in buildings: A review, *Renewable and Sustainable Energy Reviews*, 59(2016), pp. 1426-1447
- [6] E. Gratia, I. Bruyère, a De Herde, How to use natural ventilation to cool narrow office buildings, *Build Environ*, 39 (2004), pp. 1157–1170
- [7] D. Stavridou, E. Prinos, Natural ventilation of buildings due to buoyancy assisted by wind: Investigating cross ventilation with computational and laboratory simulation, *Build Environ*, 66 (2013), pp. 104–119
- [8] H.K. Versteeg, W. Malalasekera ,An introduction to Computational Fluid Dynamics, 1995
- [9] Star-CCM+ User Manual, Version 11.04, CD-adapco
- [10] N. Djongyang, R. Tchinda, D. Njomo
Thermal comfort: a review paper, *Renew Sustain Energy Rev*, 14 (9) (2010), pp. 2626–2640
- [11] Y. Cheng, J. Niu, N. Gao
Thermal comfort models: a review and numerical investigation, *Build Environ*, 47 (2012), pp. 13–22

- [12] M. Fu, W. Weng, W. Chen, N. Luo
Review on modeling heat transfer and thermoregulatory responses in human body, *J Therm Biol*, 62 (B) (2016), pp. 189–200
- [13] Huajun Zhang, Lan Dai, Guoquan Xu, Yong Li, Wei Chen, Wen-Quan Tao, Studies of air-flow and temperature fields inside a passenger compartment for improving thermal comfort and saving energy, *Applied Thermal Engineering*, Volume 29, 2009, Pages 2022-2027
- [14] Jan Fredriksson, Mats Sandberg, Bahram Moshfegh, Experimental investigation of the velocity field and airflow pattern generated by cooling ceiling beams, *Building and Environment*, Volume 36, 2001, Pages 891-899
- [15] Guo-Liang Ding, Hong-Tao Qiao, Zhi-Li Lu, Ways to improve thermal uniformity inside a refrigerator, *Applied Thermal Engineering*, Volume 24, 2004, Pages 1827–1840
- [16] B.W. Zingano, A discussion on thermal comfort with reference to bath water temperature to deduce a midpoint of the thermal comfort temperature zone, *Renewable Energy*, Volume 23, 2001, Pages 41–47
- [17] Fei Li, Junjie Liu, Jingjing Pei, Chao-Hsin Lin, Qingyan Chen, Experimental study of gaseous and particulate contaminants distribution in an aircraft cabin, *Atmospheric Environment*, Volume 85, 2014, Pages 223-233
- [18] Marco Manzan, Onorio Saro, Numerical analysis of heat and mass transfer in a passive building component cooled by water evaporation, *Energy and Buildings*, Volume 34, 2002, Pages 369–375
- [19] J.A. Khana, C.E. Feigley, E. Lee, M.R. Ahmed, S. Tamanna, Effects of inlet and exhaust locations and emitted gas density on indoor air contaminant concentrations, *Building and Environment*, Volume 41, 2006, Pages 851–863
- [20] P. Zítek, T. Vyhlídal, G. Simeunovic, L. Nováková, J. Cízek, Novel personalized and humidified air supply for airliner passengers, *Building and Environment*, Volume 45, 2010, 2345-2353

- [21] X. L. Yang, F.Z. Sun, K. Wang, Y. T. Shi, N. H. Wang, Numerical Simulation of Flow Fields in A Natural Draft Wet-Cooling Tower, *Journal of Hydrodynamics*, Volume 19, 2007, Pages 762-768
- [22] M. Bojic, M. Lee, F. Yik, Flow and temperatures outside a high-rise residential building due to heat rejection by its air-conditioners, *Energy and Buildings*, Volume 33, 2001, Pages 737-751.
- [23] Liang Pu, Yanzhong Li, Fu Xiao, Zhenjun Ma, Di Qi, Suping Shen, Effects of different inlet vent positions on the uniformity of humidity inside a building chamber, *Energy and Buildings*, Volume 76, 2014, Pages 565-571.
- [24] Jing Liu, Yoshihiro Aizawa , Hiroshi Yoshino, Experimental and numerical study on indoor temperature and humidity with free water surface, *Energy and Buildings*, Volume 37, 2005, Pages 383–388
- [25] R. Sureshkumar, S.R. Kale, P.L. Dhar, Heat and mass transfer processes between a water spray and ambient air, *Applied Thermal Engineering*, Volume 28, 2008, Pages 349–360
- [26] A. Azemati, A.Saraei, The effect of mineral micro particle in coating on energy consumption reduction and thermal comfort in a room with a radiation cooling panel in different climates, *Energy and Buildings*, Volume 82, October 2014, Pages 644-650

CURRICULUM VITAE

Graduate College
University of Nevada, Las Vegas

Armin Saraei

Email Address:

arminsaraei70@gmail.com

Degrees:

Bachelor of Science, Mechanical Engineering, 2013
Iran University of Science & Technology

Thesis Title: The Effects Exhaust Vent Location on Thermal Comfort inside the Residential Buildings Equipped with an evaporative cooling system

Thesis Examination Committee:

Chairperson, Dr. Samir F. Moujaes, Ph.D.

Committee Member, Dr. Brendan O'Toole, Ph.D.

Committee Member, Dr. William Culbreth, Ph.D.

Graduate Faculty Representative, Dr. Samaan Ladkany, Ph.D.